KINETICS AND EQUILIBRIA AT NICOTINIC RECEPTORS IN *ELECTROPHORUS ELECTRICUS* AND *RAIA ERINACEA* ELECTROPLAQUES

Thesis by

Robert Edward Sheridan, Jr.

In Partial Fulfillment of the Requirements

for the Degree of

Doctor of Philosophy

California Institute of Technology

Pasadena, California

1978

(Submitted November 1, 1977)

ACKNOWLEDGMENTS

A complete list of those who helped in the preparation of this thesis, directly or indirectly, would probably be longer than the thesis itself. Certainly the least I can do is to mention those who have aided in the most obvious ways.

First, I would like to thank Gene Pautler for introducing me to the study of neurobiology. I would like to thank Henry Lester, whose constant vigilance kept me from investigating too many dead ends. I would also like to thank Fred Sigworth for his design of the *Electrophorus* voltage-clamp circuit and Donna Williams for many, excellent *Electrophorus* electroplaques.

Finally, I would like to thank those neglected institutions without whose help much of this research would never have been begun: the National Science Foundation, the Grass Foundation, and the Spencer Foundation.

ABSTRACT

This study utilizes relaxation kinetics and equilibrium conductance to measure the response of the nicotinic receptor to cholinergic agonists. Agonist-induced conductance, postsynaptic currents (PSC's), and voltage-jump relaxations are studied in electroplaques of Electrophorus electricus. Agonist-induced conductance is instantaneously ohmic at voltages more negative than -30 mV. In bath-applied acetylcholine (ACh), the dose vs. conductance relation is sigmoid. At 15°, the apparent dissociation constant for ACh decreases e-fold for every 87 mV of hyperpolarization, hence agonist-induced conductance increases as the electroplaque is hyperpolarized. In other experiments, presynaptic terminals are stimulated to produce PSC's. Peak PSC changes linearly with membrane voltages more negative than -30 mV. The estimated reversal potential for all the above agonist-induced currents is about +10 mV. After the peak, PSC's decay with a single exponential rate, α. At 15°, α equals 1.2 $msec^{-1}$ at 0 mV and decreases e-fold for every 86 mV of hyperpolarization. In still another series of experiments, an instantaneous jump in membrane voltage causes agonist-induced conductance to relax to a new equilibrium along a simple exponential time course. The rate constant, $1/\tau$, for such relaxations varies with the nature of the agonist, its concentration, and the final membrane voltage. This relaxation rate is interpreted as the sum of the closing rate of receptors, α, and a first-order, voltage-independent rate constant for receptor opening. As expected from this interpretation: (a) $1/\tau$ approaches α at low ACh concentrations, (b) $1/\tau$ increases linearly with agonist concentration, and (c) $1/\tau$ is unaffected by blockade of

receptors with α-bungarotoxin. Several kinetic models of the nicotinic receptor are tested. The one which best fits the data assumes: (a) that the open state of the receptor forms as the receptor binds the second in a series of two agonist molecules, (b) that this process constitutes the rate-limiting step in receptor activation, and (c) that dissociation of either agonist molecule closes the receptor. In ACh, the rate-limiting step proceeds with an opening rate of 10^7 $M^{-1}sec^{-1}$ and a closing rate of 10^2 to 10^3 sec^{-1}.

Agonist-induced conductance and postsynaptic currents are also studied in electroplaques of Raia erinacea. In Raia electroplaques, delayed rectification prevents measurement of conductance at voltages more positive than -50 mV. At voltages more negative than -50 mV, bath-applied carbachol (3 to 9 μM) produces a steady-state conductance which is independent of membrane voltage. In other experiments, PSC's are produced by electrical stimulation of presynaptic nerves. Peak PSC varies linearly with membrane voltage. At 20°, the extrapolated reversal potential for all the above agonist-induced currents is about 0 mV. PSC's decay exponentially after the peak. The rate constant of the decay, α, does not vary with membrane voltage and equals 0.23 $msec^{-1}$ at 20°. This rate constant does increase with temperature and has a Q_{10} of 1.95. D-tubocurarine reduces the peak PSC but does not change the decay rate. Neostigmine reduces the decay rate but does not change the peak PSC. These results imply that the opening and closing rates of the nicotinic receptor are voltage insensitive in Raia electroplaques.

TABLE OF CONTENTS

INTRODUCTION

This study concerns the kinetics and equilibria of the nicotinic receptor's response to acetylcholine. The nicotinic receptor is a protein complex embedded in and probably extending through the postsynaptic membrane at a nicotinic synapse (Cartaud et al.,1973). The nicotinic receptor responds to acetylcholine and other cholinergic agonists by altering the postsynaptic membrane's conductance. This change in conductance is the physiologically important "product" of the reaction between acetylcholine and the nicotinic receptor. Kinetic and equilibria data are necessary for a description of any chemical reaction, and relaxation methods provide such data from physiological measurements of the nicotinic receptor response.

Relaxation methods utilize observed rates of change in a chemical system to describe the rate constants for transitions among distinct chemical states. Following a perturbation from equilibrium, a chemical system "relaxes" to a new equilibrium. For a given chemical reaction, this relaxation consists of a series of exponential decays, each of which corresponds to an eigenvalue of the matrix of rate constants for the chemical reaction. For each decay, the exponential rate constant is a simple function of the reaction rates (Kirschner et al., 1966; Eigen and deMaeyer, 1974; Hammes and Wu, 1974; Malcolm, 1975). If the transitions between two distinct chemical states are slower than transitions between the other states in the chemical reaction, the slower transitions comprise a "rate-limiting step". The rate-limiting step is associated with the slowest relaxation decay. If the

rate-limiting step is the only step slow enough to be measured, the relaxation appears to have only one decay component.

The reaction mechanism determines the relations between reaction rates and relaxation rates. Once these relations are experimentally established, hypothetical reaction mechanisms are selected for their ability to fit these experimental results. Often, more than one reaction mechanism can predict the observed kinetic data. Fortunately, the equilibrium state is a unique function of the reaction rates that, again, depends on the reaction mechanism. Thus, relations between equilibria and reaction rates provide supplemental data on the reaction mechanism.

Relaxation rates can be found without pertarbing equilibria. Spontaneous fluctuations away from equilibrium have autocorrelation functions characterized by exponential time constants. Such autocorrelation time constants equal relaxation time constants when reaction rate constants are independent of their previous history, i.e. have no "memory". This equivalence is based on the Fluctuation Dissipation Theorem (Stevens, 1972; Zingsheim and Neher, 1974). Autocorrelation time constants equal relaxation time constants for nicotinic receptors (Anderson and Stevens, 1973; Neher and Sakmann, 1975).

Nicotinic receptors undergo two reactions with agonist. The faster reaction leads to an increased agonist-induced conductance and relaxes with one decay component (Adams, 1975c; Neher and Sakmann, 1975; Sheridan and Lester, 1975, 1977). The implication is that this reaction either consists of only one step or has a distinct rate-limiting

step. The slower reaction leads to a decreased agonist-induced conductance and is called "desensitization". When nicotinic receptors are exposed to high agonist concentrations for extended periods of time, the resulting agonist-induced conductance slowly decreases. This decrease is known as desensitization (Katz and Thesleff, 1957; Magazanik and Vyskocil, 1970, 1975; Adams, 1975a; Lester et al., 1975; Scubon-Mulieri and Parsons, 1977). Desensitization occurs too slowly to affect synaptic transmission. Since the faster, physiologically significant receptor reaction does not depend on desensitization, desensitization is not of immediate interest in this study and was avoided by working at low temperatures, by applying agonists to the preparation briefly, and by permitting depolarization of the postsynaptic membrane during agonist application (Magazanik and Vyskocil, 1970, 1975). These precautions allowed measurement of nicotinic responses at equilibrium before desensitization could significantly reduce agonist-induced conductance (Sheridan and Lester, 1975). Therefore, the data reported here are probably free from artifacts associated with desensitization and represent only the faster reaction of the nicotinic receptor with agonist.

Nicotinic receptor physiology is often studied at synapses on skeletal muscle. Such preparations contain only nicotinic synapses, can be isolated <u>in vitro</u>, and have a well-defined pharmacology. Unfortunately, such skeletal muscle synapses do not allow the extremes of electrical and pharmacological manipulation that yield the most information about the nicotinic receptor. Electroplaques are analogs of muscle fibers that do not similarly limit electrical and

pharmacological manipulation.

Electroplaques are the cells which produce the electric fields found around several species of fish. Experiments in PART ONE employ electroplaques from the freshwater teleost Electrophorus electricus. Experiments in PART TWO employ electroplaques from the marine elasmobranch Raia erinacea. Both electroplaque preparations contain only nicotinic synapses, as determined by pharmacology(Brock and Eccles, 1958; Bennett, 1961; Karlin, 1967a; Lester, 1970; Ruiz-Manresa and Grundfest, 1971; Lester et al., 1975). Despite similar nicotinic pharmacology, these two preparations differ in size, shape, and extrasynaptic membrane properties and thus require somewhat different methods of physiological measurement.

Electroplaque preparations are the principle source for purified nicotinic receptor, either as postsynaptic membrane fragments or as solubilized receptor protein (Karlin and Cowburn, 1973; Weber and Changeux, 1974a,b ; Weill et al., 1974; Karlin et al., 1975; Raftery et al., 1975; Popot et al., 1976). Thus it is possible to study both receptor biochemistry and physiology on the same preparation. To date, electroplaque receptor physiology has been studied only at equilibrium (Changeux and Podleski, 1968; Karlin, 1967a; Lester et al., 1975; Moreau and Changeux, 1976). The present study expands upon these equilibrium studies and adds complementary kinetic data.

PART ONE

Studies of Cholinergic Mechanisms in *Electrophorus* Electroplaques.

MATERIALS AND METHODS

Preparation. Adult *Electrophorus electricus*, 1 to 1.5 m long, were kept in freshwater aquaria. Sections of the organ of Sachs were surgically removed from the caudal end of live animals. Five to eight such sections, each 2-3 cm thick, were removed from each fish.

Single electroplaques were dissected from a section of Sachs' organ, were cleaned of connective tissue, and were mounted in a Plexiglass chamber. Electroplaques used in these experiments were typically 3mm x 8mm x 100μm thick. The Plexiglass chamber consisted of two wells of saline separated by a partition which contained the electroplaque. Part of the electroplaque's innervated surface was exposed to one well of saline (pool A) through a 1 x 3 mm window in a sheet of mylar. The other, noninnervated, electroplaque surface was exposed to the other well of saline (pool B) through a silk screen. The electroplaque provided the only connection between pool A and pool B. (See Lester, 1977b for a detailed diagram.) Temperature was controlled by a water bath surrounding the Plexiglass chamber.

Solutions. *Electrophorus* Ringer saline contained (mM): NaCl, 160; KCl, 2.5; $CaCl_2$, 2; $MgCl_2$, 2. The Ringer saline was buffered with either 5 mM phosphate (pH 6.9) or 10 mM HEPES (pH 7.3). The HEPES buffer was preferred for its greater buffering capacity. The two buffers gave identical experimental results.

Solutions in pool B contained 6 mM glucose. Solutions in pool A

contained a variety of drugs in addition to the Ringer saline. All pool A solutions contained 3 mM $BaCl_2$ to maintain the anomalous K^+ rectifier in a low-conductance state (Ruiz-Manresa et al., 1970). Electrophorus electroplaques have no delayed K^+ conductance. During measurement of responses to bath-applied agonists, the electrically excitable Na^+ conductance was blocked with 10^{-7} to 10^{-6} M tetrodotoxin (TTX) added to pool A, and acetylcholinesterase was irreversibly inhibited either with 10 mM methanesulfonyl fluoride (MSF) or with 0.4 mM diisopropyl fluorophosphate (DFP) added to pool A for 30 to 50 min at 20°. During solution changes, 10 ml of replacement solution were flushed through pool A (0.7 ml capacity) in 10 to 20 sec.

Electrical Arrangements. Voltage-clamp circuits were used to measure the conductance of the innervated membrane. Voltage across the innervated membrane was measured in either of two ways. The first method used a pair of 5-10 megohm microelectrodes which straddled the innervated membrane (Nakamura et al., 1965; Lester et al., 1975). The second method used a 200 kilohm, extracellular electrode in pool A (V_3); a 200 kilohm, extracellular electrode in pool B (V_1); and a 5-10 megohm, intracellular microelectrode (V_2). The resting potential, $(V_1 - V_2)_o$, was electronically stored shortly before the voltage-clamp feedback loop was closed. Later, during current flow in the voltage-clamp circuit, the computed voltage across the noninnervated membrane, IZ, and the stored resting potential were subtracted from the voltage across the entire electroplaque, $V_1 - V_3$. Thus, the second method calculated the innervated membrane's voltage as:

$V_1 - V_3 - IZ - (V_1 - V_2)_o$. Both methods were corrected for series resistance by subtracting IR_s where R_s is the series resistance due to Ringer solution (Lester, 1977b; Sheridan and Lester, 1977). In both voltage-clamp circuits, current applied to a Pt plate in pool B passed through the electroplaque to a virtual ground current monitor via a Pt plate in pool A. Both voltage-clamp circuits gave equivalent results for slowly changing conductances. However, the second voltage-clamp circuit allowed 3-fold faster measurement of membrane current (time constants of 50 μsec as opposed to 170 μsec). Therefore, the second voltage-clamp circuit was used in a majority of these experiments.

All the analog circuits described above were controlled by command voltages from a digital minicomputer (Data General Corporation, Nova 2/10). Voltage across the innervated membrane and current at the virtual ground were digitized by the computer and stored on magnetic tape for later analysis. Currents were scaled to the mylar window's area.

EQUILIBRIUM RESPONSES TO CHOLINERGIC AGONISTS.

Chord Conductance. Chord conductance, g_j, equals $I_j/(V - E_j)$, where E_j is the potential at which current flowing through the j pathway, I_j, reverses polarity (Hodgkin and Huxley, 1952). In practice, g_j is often measured by eliminating or subtracting all but the I_j current. The remaining current is then a linear measure of g_j at a given voltage. However, because chord conductance is often a function of membrane voltage, only the chord conductance can be used for comparison of responses at different voltages.

Membrane Properties. Intact Electrophorus electroplaques had resting potentials of -80 to -90 mV. These electroplaques had Na^+ action potentials of 120 to 180 mV amplitude. In order to measure leakage of current around the electroplaque, the intracellularly and transcellularly recorded Na^+ action potential amplitudes were compared. Preparations were used when these amplitudes agreed to within 20%. After addition of Ba^{++} and TTX, the innervated membrane had a linear current vs. voltage relation from -200 mV to +100 mV (Figure 1). This "passive" membrane conductance averaged 41 ± 3 mmho/cm^2 (mean ± SEM, 12 cells). Passive membrane current reverses polarity at the resting potential. Neither Ba^{++} nor TTX changed the resting potential.

Measurement of Agonist-Induced Conductance. Bath-applied, cholinergic agonists depolarize the innervated membrane of Electrophorus electroplaques (Schoffeniels and Nachmanson, 1957). This depolarization results primarily from a slow, positive going "shift" in the reversal potential for passive current (Karlin, 1967b; Lester et al., 1975; Lester, 1977a). Passive membrane conductance does not change in response to bath-applied agonist. The agonist-induced shift in passive current reversal potential normally disappears after agonist is removed but becomes permanent if the electroplaque is pretreated with ouabain or strophanthidin (Lester et al., 1975).

In order to measure agonist-induced conductance, passive current must be subtracted from membrane current during exposure to agonist. This subtraction is complicated by the variable shift of the passive membrane's current vs. voltage relation during agonist application.

Figure 1. Equilibrium current vs. voltage relations in Electrophorus electroplaques. Upper curve: passive membrane current before agonist. Lower curve: membrane current in 150 μM carbachol. Light line: estimated values of the "shifted" passive membrane current in carbachol. Currents were obtained by continuously changing the membrane voltage at a rate of 0.8 V/sec. Temperature, 15°.

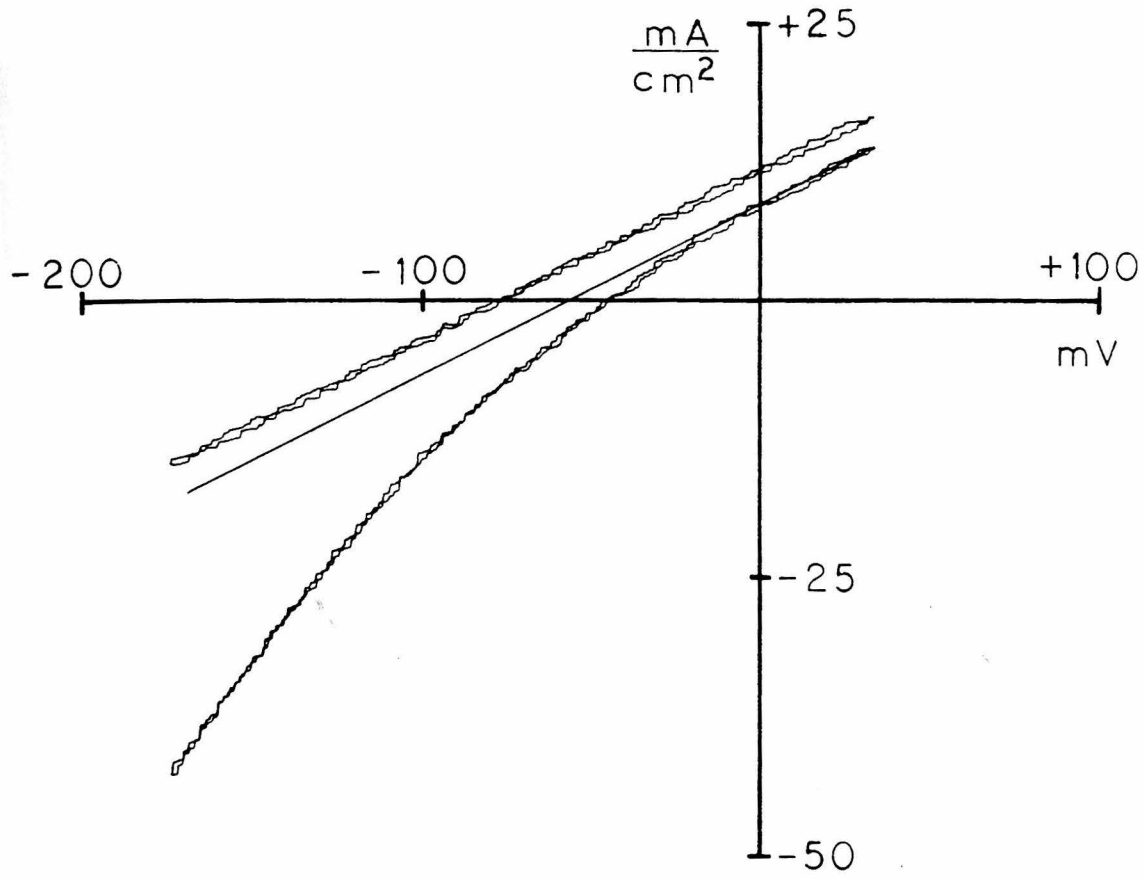
mA
cm²
+25
-25
-50
-200
-100
+100
mV

Fortunately, agonist-induced current is a nonlinear function of membrane voltage. At voltages more positive than about 0 mV, agonist-induced current is essentially zero, and only the "shifted" passive current remains. Since the passive current vs. voltage relation is linear, the complete passive current vs. voltage relation, with shift, can be generated by linear extrapolation from membrane current at positive voltages (Figure 1). This procedure has been verified using ouabain or strophanthidin treated electroplaques (Lester et al., 1975).

Instantaneous Agonist-Induced Current. Agonist-induced conductance is a function of membrane voltage and time. Immediately following an "instantaneous" jump in membrane voltage from some voltage V to another voltage V', agonist-induced conductance is determined by equilibrium conditions at V. The agonist-induced conductance then gradually approaches equilibrium conditions at V'. Starting with a measurable conductance at V, instantaneous and equilibrium currents at V' will be equal only when V' equals the reversal potential, E.

For voltages more negative than -30 mV, instantaneous agonist-induced current increases linearly as membrane voltage becomes more negative (Figure 2). At voltages more positive than -30 mV, agonist-induced current changes less than linearly with voltage. As a result, the intercept of instantaneous and equilibrium current was difficult to determine except by extrapolation from negative voltages. Such extrapolations yielded an average reversal potential for agonist-induced current at 15° of +10 mV with a range of 0 to +20 mV.

Figure 2. Current vs. voltage relations in 75 μM acetylcholine. Filled circles: equilibrium agonist-induced currents. Open circles: instantaneous agonist-induced currents. The asterisk indicates the equilibrium current before the voltage jumped to a more positive value. The reversal potential is the extrapolated intercept of the instantaneous and equilibrium currents (-5 mV). Temperature, 9°.

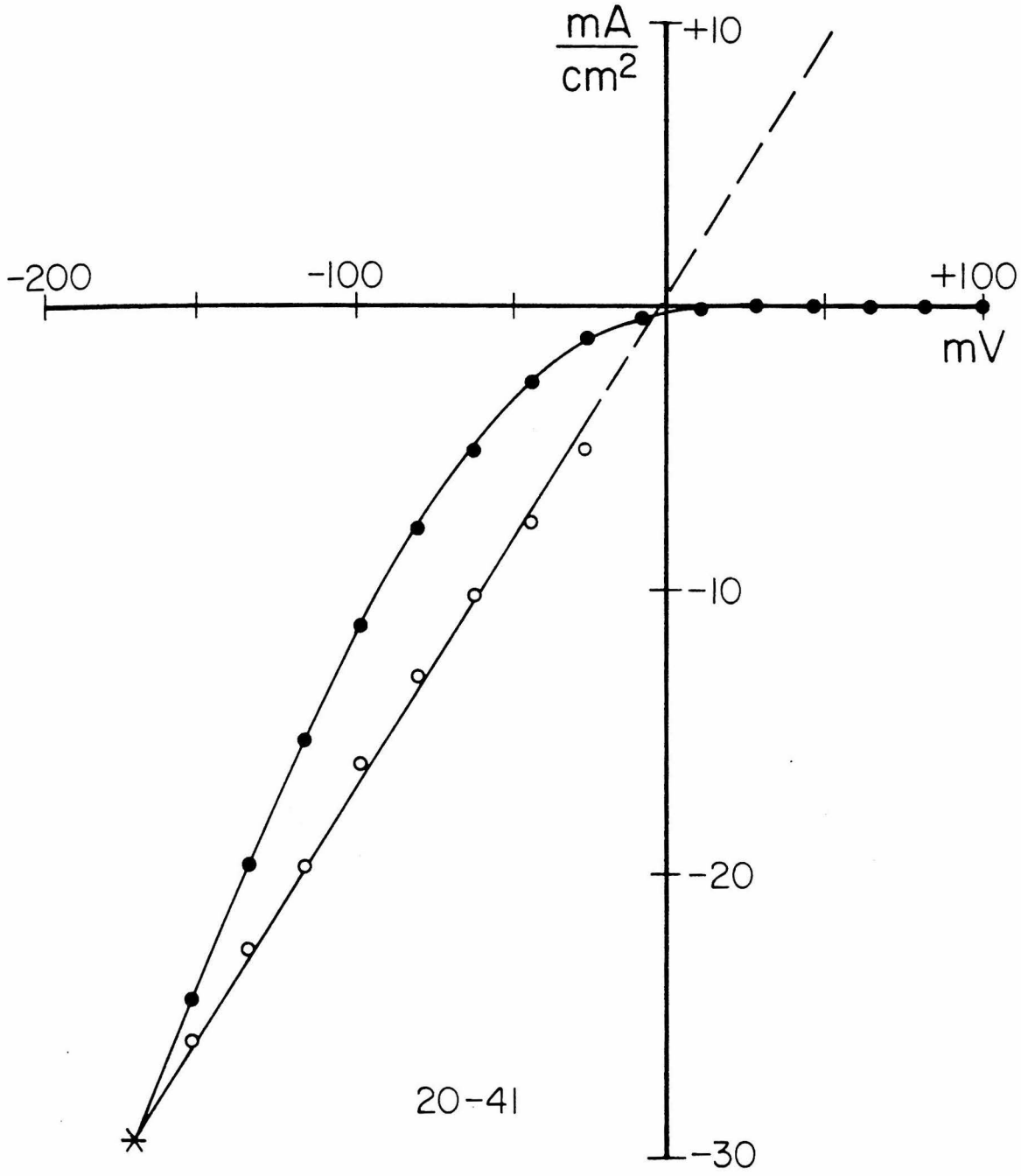
mA
cm²
+10
-200
-100
+100
mV
-10
-20
-30
20-41

Slightly more negative reversal potentials are found during iontophoretic application of agonist at higher temperatures (Lassignal and Martin, 1976, 1977). There are several possible explanations for the nonlinear relation between instantaneous, agonist-induced current and membrane voltage. First, if nicotinic receptor kinetics increase markedly at positive voltages, the voltage jump may be too slow to be considered instantaneous at voltages more positive than -30 mV. Second, nicotinic receptors could rectify against the passage of outward current. In either case, agonist-induced conductance is instantaneously ohmic at voltages more negative than -30 mV. A similar, instantaneously ohmic conductance is found at nicotinic synapses on amphibian skeletal muscle (Magleby and Stevens, 1972a; Dionne and Stevens, 1975).

Voltage Dependence of Agonist-Induced Conductance. At equilibrium, agonist-induced conductance increases as membrane voltage becomes more negative (Figure 3). For low agonist concentrations (i.e. 7.5 μM acetylcholine) and for voltages in the range of instantaneously ohmic conductance (more negative than -30 mV), the equilibrium, agonist-induced conductance increases exponentially as membrane voltage becomes more negative. The agonist-induced conductance changes e-fold for each 87 ± 10 mV (mean ± SD, 6 cells) at 15°. Similar voltage sensitivity is found during agonist application to amphibian skeletal muscle (Dionne and Stevens, 1975; Adams, 1975b, 1976). For high agonist concentrations (i.e. greater than 20 μM acetylcholine) the equilibrium, agonist-induced conductance increases less than

Figure 3. Semilogarithmic plot of agonist-induced conductance vs. membrane voltage at equilibrium.
Filled triangles: 7.5 μM acetylcholine.
Open circles: 20 μM acetylcholine.
Filled circles: 50 μM acetylcholine.
Temperature, 15°.

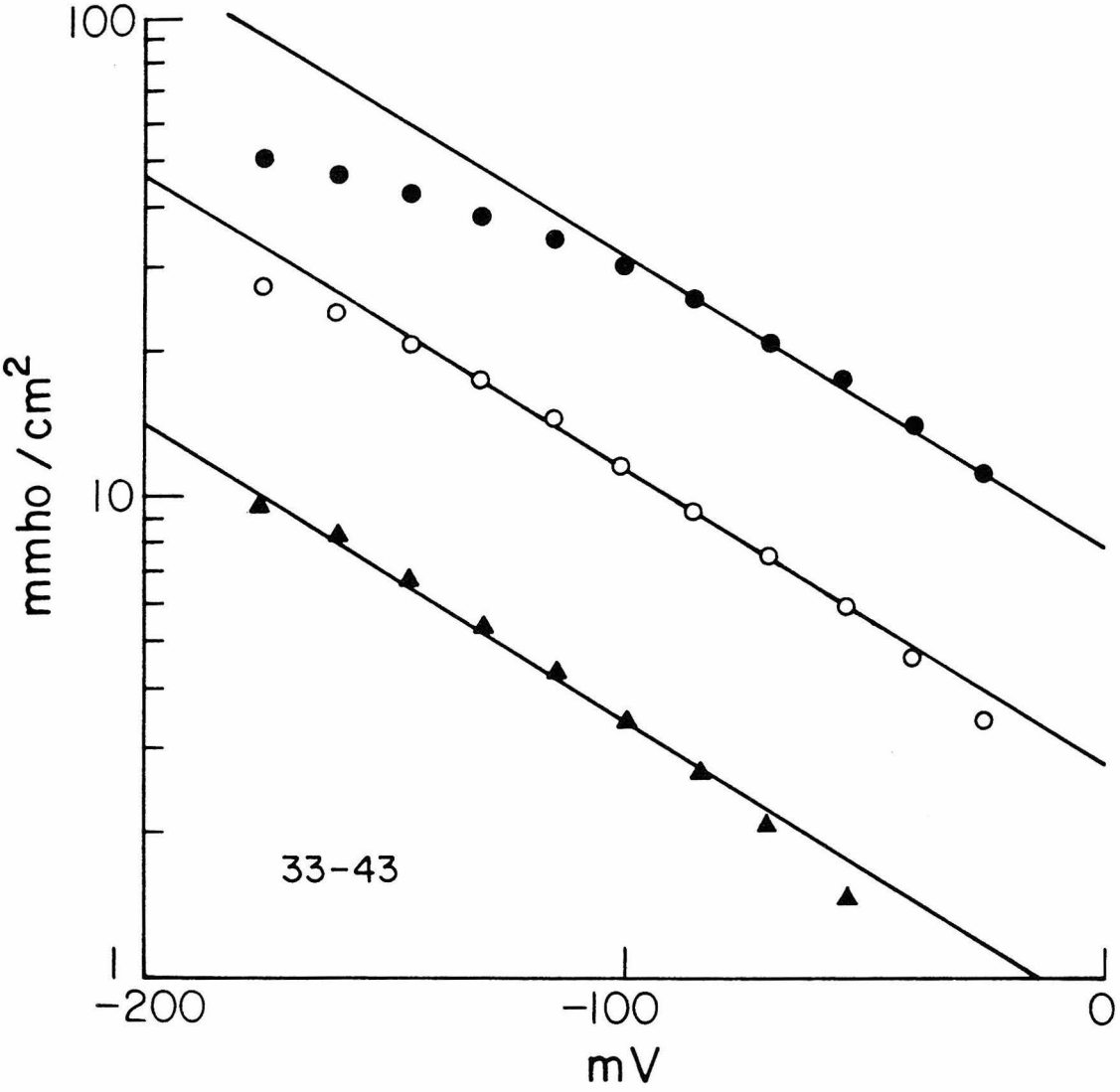
100
10
1
mmho / cm²
33-43
−200
−100
0
mV

exponentially at negative voltages. The higher the agonist concentration, the less negative the voltage where deviation from exponential voltage sensitivity occurs. At very high agonist concentrations and at negative voltages, agonist-induced conductance becomes nearly constant with voltage. These high agonist concentrations have not been studied in amphibian skeletal muscle due to limitations of that preparation.

Dose vs. Conductance Relations. At any given voltage, higher agonist concentrations produce larger equilibrium conductances (Figure 4). At equilibrium, agonist-induced conductance increases more than linearly with low agonist concentrations and less than linearly with high agonist concentrations. At very high agonist concentrations the equilibrium conductance approaches a maximum value, $r\gamma$. This maximum conductance can be viewed as being the response of r receptors, each having a conductance of γ. Similarly sigmoid dose vs. response relations have been found in amphibian skeletal muscle (Adams, 1975b; Dreyer and Peper, 1975a,b) as well as in Electrophorus electroplaque (Karlin, 1967a; Changeux and Podleski, 1968; Lester et al., 1975).

The first bath application of agonist consistently results in larger conductances than subsequent applications of the same concentration. Although the reasons for this effect are unknown, the effect can be circumvented by using only the second and subsequent agonist applications to construct dose vs. conductance curves, such as those of Figure 4. Such data were repeatable within a given electroplaque.

In Figure 4, the continuous curves were fit to the data points according to the equation:

Figure 4. Equipotential dose vs. conductance curves for acetylcholine. Double logarithmic plot of equilibrium, agonist-induced conductance vs. acetylcholine concentration. Fitted curves are from equation (1) with K_{app} indicated by a dashed line. Experimental uncertainty was approximately 0.12 mmho/cm^2. Temperature, 15°.

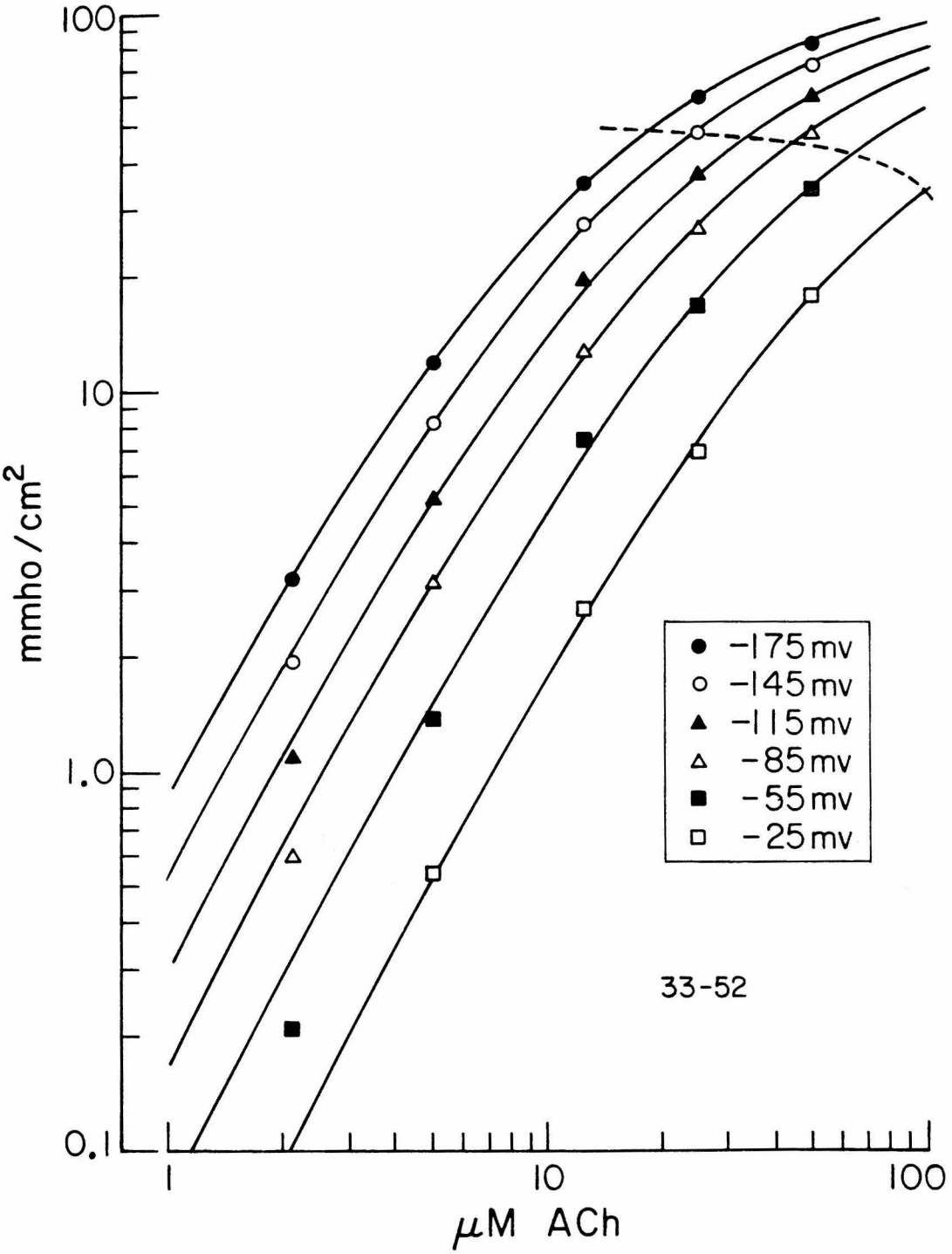
100
10
1.0
0.1
mmho/cm²
1
10
100
μM ACh
● -175 mv
○ -145 mv
▲ -115 mv
△ -85 mv
■ -55 mv
□ -25 mv
33-52

$$g = r\gamma(A/(A + 0.414K_{app}))^2 \qquad (1)$$

where A is the acetylcholine concentration and K_{app} is the concentration at half-maximal conductance. The Hill coefficient equals the slope of the double logarithmic plot of dose vs. $(g/(r\gamma - g))$. For small agonist-induced conductances, the double logarithmic plot of dose vs. conductance has a slope approximately equal to the Hill coefficient (Dreyer and Peper, 1975a; Fromm, 1975). In bath-applied acetylcholine the Hill coefficient averaged 1.9 and ranged from 1.8 to 2.0. Since desensitization is faster and more pronounced at higher agonist concentrations, not only the maximum agonist-induced conductance but also the Hill coefficient could have been reduced by desensitization during bath application. However, a Hill coefficient of 2 is consistently found for acetylcholine and carbachol responses at nicotinic receptors (Karlin, 1967a; Changeux and Podleski, 1968; Adams, 1975b; Lester et al., 1975). Two notable exceptions are Dreyer and Peper (1975a), who found a Hill coefficient of approximately 3.0 at amphibian skeletal muscle endplate, and Moreau and Changeux (1976), who found a Hill coefficient of approximately 1.0 in Torpedo marmorata electroplaques. These latter two measurements rely on theoretical assumptions which may not be valid in the preparations chosen. It should be noted that all these estimates of the Hill coefficient are based on physiological responses of the nicotinic receptor. Biochemical studies of agonist binding indicate much lower Hill coefficients, ranging from 1.0 (Raftery et al., 1975) to 1.3 (Weber and Changeux, 1974b; Changeux et al., 1975).

Figure 5. Voltage dependence of the apparent dissociation constant for acetylcholine. Semilogarithmic plot of K_{app} vs. membrane voltage for the data of Figure 4. Continuous line indicates an e-fold change for 91 mV. Temperature, 15°.

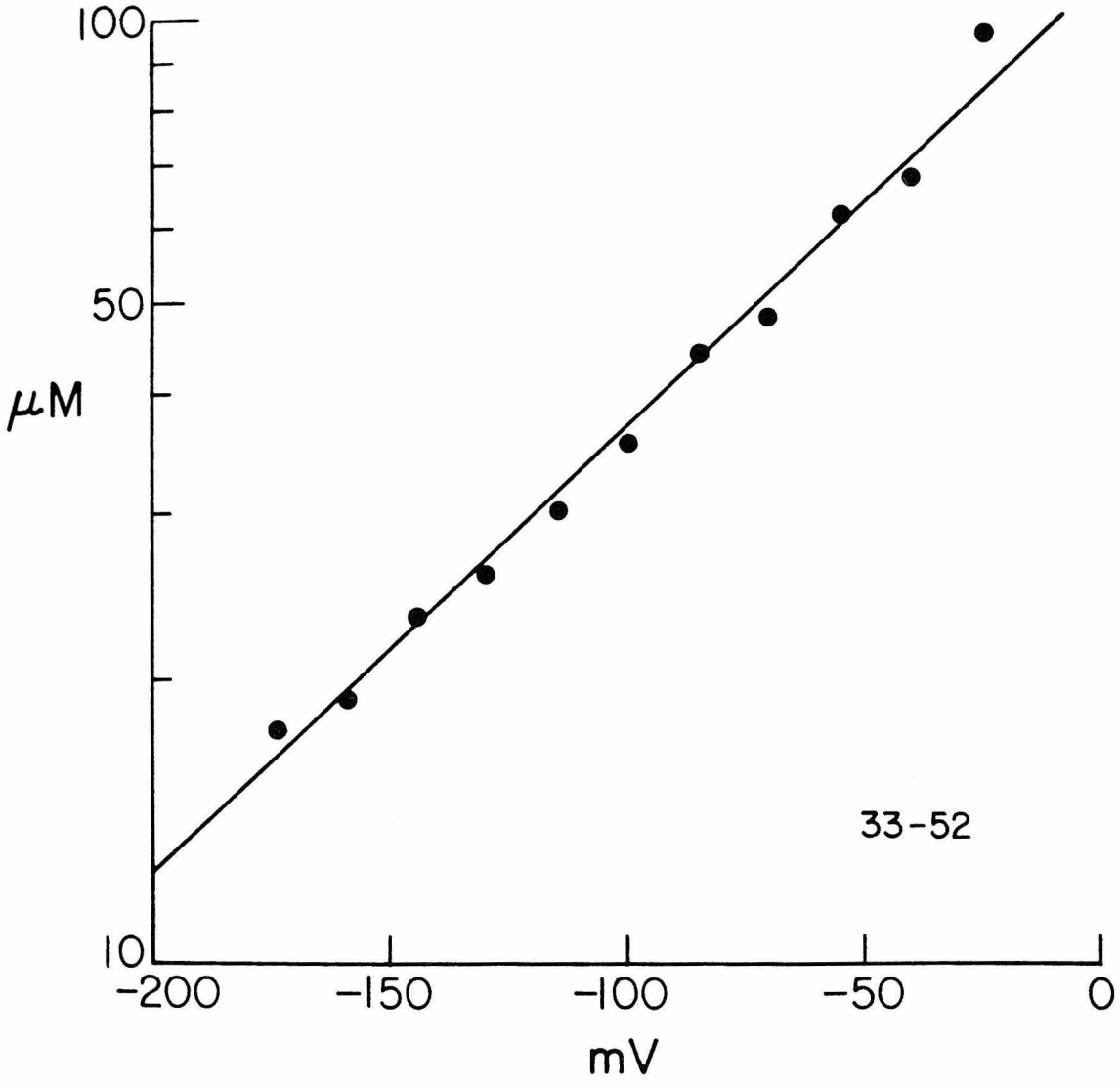
100
50
10
μM
33-52
-200
-150
-100
-50
0
mV

When membrane voltage is changed, the dose vs. conductance relation shifts along the concentration axis without changing its shape (Figure 4). The maximum agonist-induced conductance, $r\gamma$, is essentially constant for voltages more negative than -30 mV. At voltages more positive than -30 mV, $r\gamma$ decreases slightly (Figure 4). Like instantaneous, agonist-induced conductance, the voltage dependence of $r\gamma$ could result from instantaneous rectification. However, the principal effect of voltage is to change the apparent dissociation constant, K_{app}. As membrane voltage becomes more positive, K_{app} increases exponentially (Figure 5). The apparent dissociation constant for acetylcholine increases e-fold for every 87 ± 4 mV (mean ± SD, 4 cells) at 15°. Assuming that the only significant effect of membrane voltage is to change K_{app}, voltage can be viewed as moving the equilibrium dose vs. conductance curve with respect to a fixed agonist concentration. This interpretation accounts for the voltage dependence of equilibrium conductance in both low and high agonist concentrations (see Figure 3).

NEURALLY EVOKED POSTSYNAPTIC CURRENTS

Generation of Neurally Evoked Postsynaptic Currents (PSC's). In the Electrophorus electroplaque preparation, presynaptic nerves cannot be stimulated with a separate electrode. Therefore, presynaptic nerve terminals were stimulated with a large, brief current pulse through the electroplaque's innervated surface. A portion of this current flows through the presynaptic terminals and depolarizes part of the terminals' membrane. Electrically excitable currents then propagate

the depolarization throughout each terminal and lead to acetylcholine release. Since electrically excitable currents must be functional in the presynaptic terminals, TTX could not be applied in the bath. Sodium action potentials were avoided in the electroplaque by inactivating the sodium conductance with a brief depolarization prior to stimulation of the PSC (Hodgkin and Huxley, 1952). PSC's are sufficiently brief that neither desensitization nor shift in the reversal potential for passive current occur. Thus PSC's can be isolated from passive membrane currents simply by subtracting voltage-clamp currents in the absence of the current pulse which stimulates the PSC. Every measured PSC series was preceded by ten stimulations (at 3/sec) which brought acetylcholine release to a constant level of facilitation. Unless stated otherwise, all PSC's were obtained in electroplaques with functional acetylcholinesterase.

Peak PSC vs. Voltage. Electrophorus electroplaques have a linear peak PSC vs. voltage relation at voltages more negative than -30 mV. At more positive voltages the peak PSC changes less than linearly with voltage (Figure 6). By contrast, in amphibian skeletal muscle fibers, the peak PSC increases less than linearly as voltage becomes more negative and more than linearly as voltage becomes more positive (Kordas, 1968; Magleby and Stevens, 1972b; Dionne and Stevens, 1975).

Several explanations are possible for the nonlinear dependence of peak PSC on voltage in Electrophorus electroplaques. First, presynaptic stimulation could produce asynchronous release of acetylcholine, resulting in proportionately greater reductions in peak

Figure 6. Reversal of the peak PSC in a preparation treated with MSF to inhibit acetylcholinesterase. Reversal occurred at +14 mV. Insert shows PSC's. Temperature, 15°.

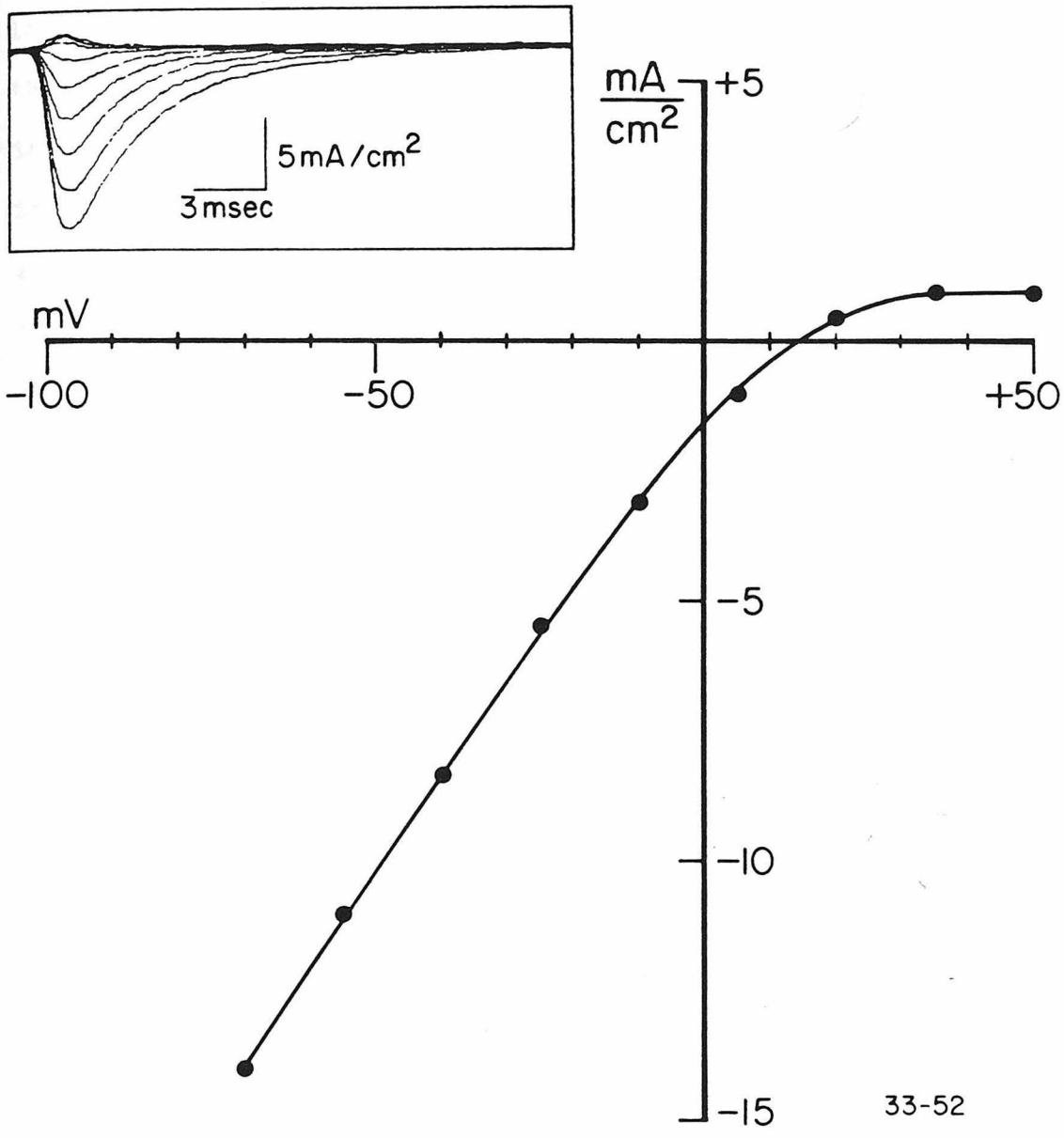
5mA/cm2
3msec
mA
cm2
+5
mV
-100
-50
+50
-5
-10
-15
33-52

PSC among the briefer PSC's at positive voltages. (See the following sections for details.) Second, the peak PSC could be an equilibrium state like the agonist-induced currents in bath-applied or iontophoretically applied acetylcholine. In support of this explanation, the agonist-induced current is similarly voltage dependent during iontophoretic application of agonist in amphibian skeletal muscle and in Electrophorus electroplaque, during bath application of agonist in amphibian skeletal muscle and in Electrophorus electroplaque, and during peak PSC in Electrophorus electroplaque (Dionne and Stevens, 1975; Dreyer and Peper, 1975a,b; Adams, 1975a, 1976; Lassignal and Martin, 1976, 1977; Lester et al., 1975; Sheridan and Lester, 1975, 1977). Third, nonlinear peak PSC vs. voltage relations could arise from instantaneous rectification against the passage of outward current by the nicotinic receptor. Like the peak PSC, instantaneous agonist-induced current and maximum agonist-induced conductance are reduced at voltages more positive than -30 mV. Such rectification would imply significant differences between nicotinic receptors in Electrophorus electroplaques and nicotinic receptors in amphibian skeletal muscle fibers, where no rectification at positive voltages has been observed.

The reversal potential for peak PSC is a measure of the reversal potential for equilibrium agonist-induced current, E. Peak PSC's actually reversed polarity in only 40% of the electroplaques studied, usually after acetylcholinesterase inhibition (Figure 6). The reversal potential for peak PSC's was +10 $\pm$ 2 mV (mean $\pm$ SEM, 6 cells) at 15° in those electroplaques which did show reversal. The same average

reversal potential was obtained from instantaneous agonist-induced currents. The PSC reversal potential was not changed by the presence of $BaCl_2$ in the bath (pool A).

The maximum conductance during a PSC was only 13 ± 6 % (mean ± SEM, 6 cells) greater than the maximum conductance induced by bath application of acetylcholine to the same electroplaques. This similarity suggests that the same receptor population is stimulated by bath-applied acetylcholine and by neurally evoked acetylcholine release. Moreover, if this small difference in maximum agonist-induced conductance is due to desensitization, then desensitization reduced agonist-induced conductance by less than 13% during bath applications.

PSC Waveform. Postsynaptic currents rapidly increase to a peak and then decay exponentially (Figure 7). The PSC "growth time" was measured as the time from 20% to 80% of the peak PSC. The PSC growth time lasts 735 ± 54 μsec (mean ± SD, 14 measurements) at 15° and changes less than 10% with membrane voltages from 0 to -175 mV. For comparison, extracellularly recorded, spontaneous, miniature PSC's have a growth time of 160 ± 55 μsec (mean ± SD, 34 measurements) at 23° and -90 mV. These values agree with PSC and miniature PSC growth times in amphibian skeletal muscle (Gage and McBurney, 1975; Gage, 1976). PSC decay begins with a small (<5%), nonexponential component which may be considered to be part of the PSC peak. The rest of the PSC decay follows a simple exponential time course through more than 95% of the return to baseline (Figure 7b). For consistency with the terminology of Magleby and Stevens (1972a,b) for the same process in amphibian skeletal

Figure 7. Neurally evoked PSC's. (a) Superimposed PSC's at membrane voltages from +5 mV (number 1) to -175 mV (number 13) in 15 mV increments. (b) Semilogarithmic plot of PSC decays. Only the linear portions of the plot are used to calculate the decay rate constant. Same time axis applied to (a) and (b). Reversal potential was +14 mV. Passive conductance of the electroplaque was 91 mmho/cm^2. Temperature, 15°.

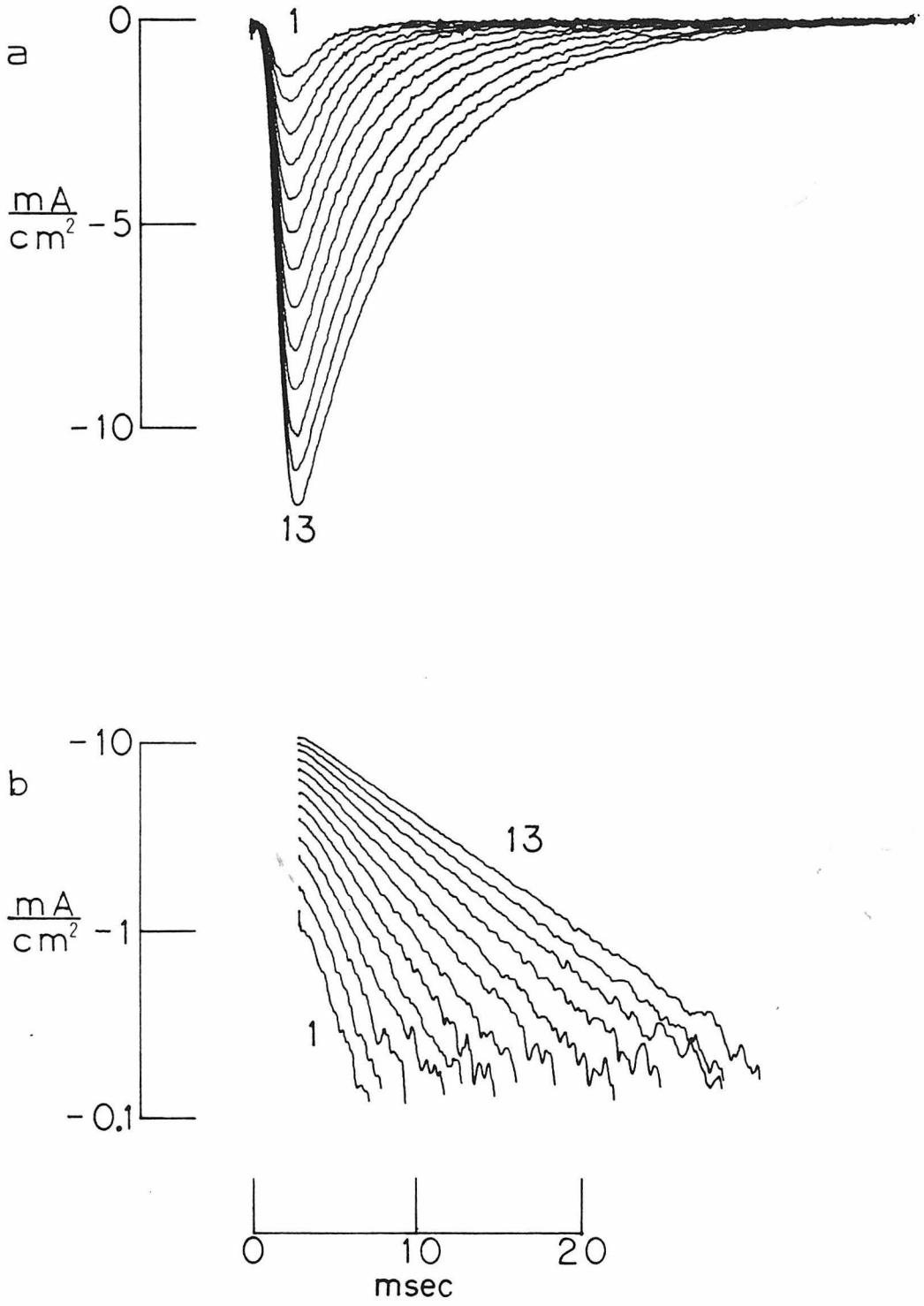
a
0
-5
-10
mA/cm²
1
13
b
-10
-1
-0.1
mA/cm²
13
1
0
10
20
msec

muscle, the exponential PSC decay rate constant will be called α.

Changing the PSC Decay Rate. The PSC decay rate can be changed with certain drugs. The PSC decay rate is reduced approximately 60% upon acetylcholinesterase inhibition with MSF or DFP. Under these conditions, the additional application of d-tubocurarine (1 to 4 μM) increases the PSC decay rate. The PSC decay rate can be increased in this manner to within 10% of the PSC decay rate before acetylcholinesterase inhibition. When acetylcholinesterase is not inhibited, d-tubocurarine has no effect on the time course of the PSC. Comparable results have been obtained in amphibian skeletal muscle (Katz and Miledi, 1973). The presence of $BaCl_2$ in pool A has little (<10%) effect on the PSC decay rate constant in Electrophorus electroplaques.

The rate constant of PSC decay, α, increases as the electroplaque's temperature is increased. At -175 mV, α has a Q_{10} of 3.2. The same Q_{10} is found for PSC decay rates in amphibian skeletal muscle fibers at similar voltages (Magleby and Stevens, 1972b; Kordas, 1972b). In amphibian skeletal muscle the Q_{10} of α decreases as the membrane voltage becomes more positive (Magleby and Stevens, 1972b). This phenomenon has not been investigated in Electrophorus electroplaques.

The rate constant of PSC decay, α, increases exponentially as membrane voltage becomes more positive (Figure 8). The relation of α to membrane voltage is:

$$\alpha = \alpha_0 \exp (V/V_1) \qquad (2)$$

for all voltages between 0 and -175 mV. At 15°, α_0 is 1.23 ± 0.12 $msec^{-1}$ (mean ± SEM, 7 cells) and V_1 is 86 ± 6 mV (mean ± SEM, 7 cells).

Figure 8. Semilogarithmic plot of PSC decay rate constants vs. membrane voltage. Line corresponds to an e-fold change for 84 mV. Same electroplaque as Figures 4 and 5. Temperature, 15°.

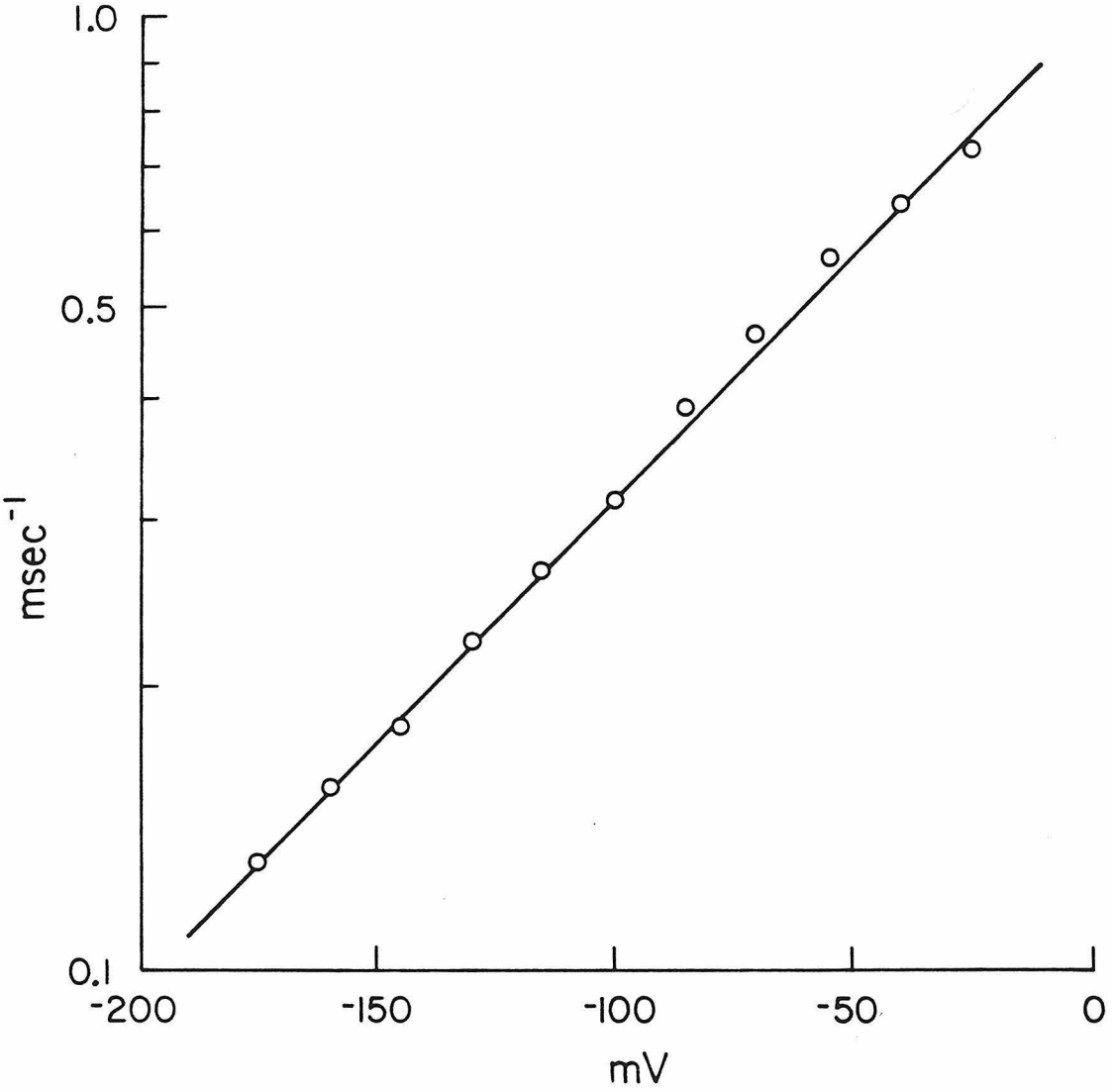
1.0
0.5
0.1
msec^{-1}
-200
-150
-100
-50
0
mV

Since the growth time for PSC's is essentially independent of voltage, the increased decay rate at positive voltages has the effect of shortening the duration of the PSC at positive voltages. The constant V_1 increases to approximately 120 mV at 22°. Similar values of V_1 are found for the PSC decay in amphibian skeletal muscle (Magleby and Stevens, 1972a,b; Kordas, 1972a,b; Gage and McBurney, 1975). In Electrophorus electroplaques, a number of receptor processes have the same voltage dependence. These processes include: (a) the PSC decay rate, (b) the equilibrium conductance in low acetylcholine concentrations, and (c) the apparent dissociation constant of acetylcholine. All of these processes vary e-fold for each 85 to 90 mV at 15°.

Interpretation of PSC Decay Rates. In amphibian skeletal muscle, the PSC decay rate is thought to represent the "closing" rate of nicotinic receptors (Magleby and Stevens, 1972a,b; Kordas, 1972a,b; Anderson and Stevens, 1973). It is thought that neurally released acetylcholine is eliminated from the synaptic cleft by hydrolysis and/or diffusion before the end of the PSC peak, and the PSC decay is thus a relaxation from a population of "open" receptors (in a high conductance state) to a population of "closed" receptors (in a low conductance state). Furthermore, since the acetylcholine concentration is zero during the PSC decay, the "opening" rate of receptors is zero and the PSC decay rate represents only the closing rate.

In amphibian skeletal muscle, several indirect observations support this argument that the PSC decay rate equals the closing rate of nicotinic receptors. (a) PSC decay is always a simple exponential

and therefore probably represents one molecular process. (b) The PSC decay rate is too temperature dependent to be a diffusion limited process (Magleby and Stevens, 1972b; Kordas, 1972b; Gage and McBurney, 1975). (c) The PSC decay rate constant is a simple function of postsynaptic membrane voltage, indicating that the PSC decay rate is governed by a process at the postsynaptic membrane (Magleby and Stevens, 1972a; Kordas, 1972a; Gage and McBurney, 1975). (d) D-tubocurarine does not shorten the PSC decay when acetylcholinesterase is not inhibited, indicating that acetylcholine is not present in the synaptic cleft during PSC decay (Katz and Miledi, 1973). (e) Acetylcholine-induced spontaneous fluctuations indicated a mean channel lifetime equal to the inverse PSC decay rate constant (Katz and Miledi, 1972; Anderson and Stevens, 1973; Colquhoun et al., 1977).

Most of these observations have been confirmed in Electrophorus electroplaques. For example, in Electrophorus electroplaques, PSC decays are (a) as exponential, (b) as temperature dependent, (c) as voltage dependent, and (d) as insensitive to d-tubocurarine as are PSC decays in amphibian skeletal muscle. To the extent that these observations support the equivalence of PSC decay rate and the closing rate for nicotinic receptors in amphibian skeletal muscle, the Electrophorus electroplaque's PSC decay rate also equals the closing rate for nicotinic receptors. However, agonist-induced spontaneous fluctuations have never been studied in Electrophorus electroplaques. Thus, this single, strongest observation supporting the equivalence of PSC decay rates and closing rates for nicotinic receptors is lacking in Electrophorus electroplaques.

VOLTAGE-JUMP RELAXATIONS

Generation of Voltage-Jump Relaxations. At equilibrium, agonist-induced conductance changes with membrane voltage (Figure 3). However, agonist-induced conductance is instantaneously ohmic at voltages between -30 and -175 mV (Figure 2). Therefore, an instantaneous jump in membrane voltage perturbs equilibrium and results in a relaxation of agonist-induced conductance. Since such "voltage-jump relaxations" occur in the presence of agonist, voltage-jump relaxation rates, unlike PSC decay rates, reflect both opening and closing rates of the nicotinic receptor. At any given voltage and time, agonist-induced current is a linear measure of agonist-induced conductance and was used, instead of conductance, to determine voltage-jump relaxation rates.

The nonlinear relation of agonist-induced current and voltage suggests two, essentially similar, protocols for generating voltage-jump relaxations. Both protocols yield identical experimental results, and in both protocols $BaCl_2$ and TTX are applied to make the electroplaque's passive current vs. voltage relation linear.

The first protocol involves recording a series of control voltage jumps without agonist. These voltage-jump currents measure passive membrane conductance and membrane capacitance. The same voltage jumps are repeated in bath-applied agonist. The "control" voltage-jump currents are then subtracted from the "agonist" voltage-jump currents. The resulting agonist-induced current is then corrected for shift in the passive current vs. voltage relation during exposure to agonist. Specifically, the difference between control and agonist voltage-jump

Figure 9. Voltage-jump relaxations in 25 μM acetylcholine. (a) Superimposed traces of membrane voltage. Second voltage level is changed for each episode. (b) Agonist-induced currents. Passive conductance and capacitative currents have been subtracted (see text). (c) Semi-logarithmic plot of the approach to steady state in the lower six traces of (b). Points start 180 μsec after the voltage jump. Time axis applies to all three panels. Temperature, 14°.

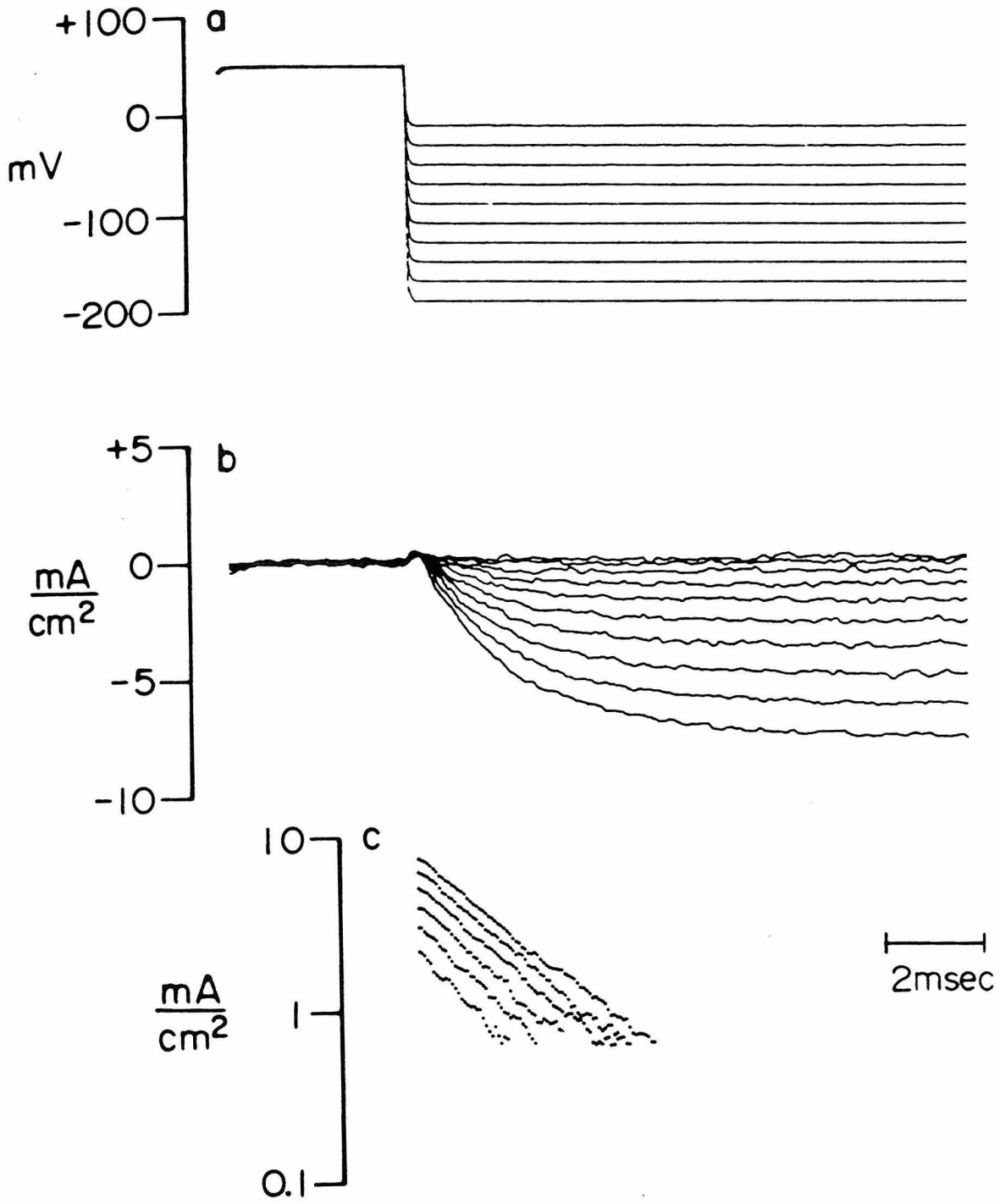
+100
a
0
mV
-100
-200
+5
b
mA
cm²
0
-5
-10
10
c
mA
cm²
1
0.1
2msec

currents is adjusted to give an agonist-induced current of zero at voltages more positive than 0 mV (Figure 9). Under most circumstances this protocol works satisfactorily. However, the protocol assumes that passive conductance is constant with voltage and time. Since the passive conductance can change over the time course of the experiment, this assumption can result in errors during subtraction of control from agonist voltage-jump currents.

The second protocol for voltage-jump relaxations relies only on the linearity of passive current and of capacitance with voltage. The electroplaque undergoes two types of voltage jump in bath-applied agonist. The first voltage jump occurs exclusively at positive voltages, where agonist-induced conductance is negligible. A second voltage jump occurs at more negative voltages, where agonist-induced conductance is significant. Then the first voltage-jump currents are scaled and subtracted from the second voltage-jump currents, leaving the agonist-induced current (Figure 10). Like the first protocol, the subtracted currents are adjusted to have a zero value at voltages more positive than 0 mV. Because both passive and agonist-induced currents are measured at the same time, this protocol is free of problems associated with slow changes in passive conductance. However, this second protocol has two problems not found in the first protocol. First, voltage jumps at positive voltages must be smaller than voltage jumps at negative voltages to avoid breakdown of the membrane dielectric. Therefore, passive currents must be multiplied before subtraction. This procedure increases the noise in the resulting agonist-induced currents. Second, this protocol measures the gating

Figure 10. Voltage-jump relaxations in 50 μM acetylcholine. Averaged records from two identical experiments, each consisting of 16 episodes (numbered 1 to 16). (a) Membrane voltages during each episode. (b) Membrane currents during the same episodes. Currents during the first half of each episode are essentially passive. Currents during the second half of each episode contain agonist-induced current. (c) Agonist-induced currents obtained by scaling and adding the two halves of each episode (see text). (d) Semilogarithmic plot of approach to steady state for the last eight episodes in (c). Same time axis applies to all panels. Temperature, 15°.

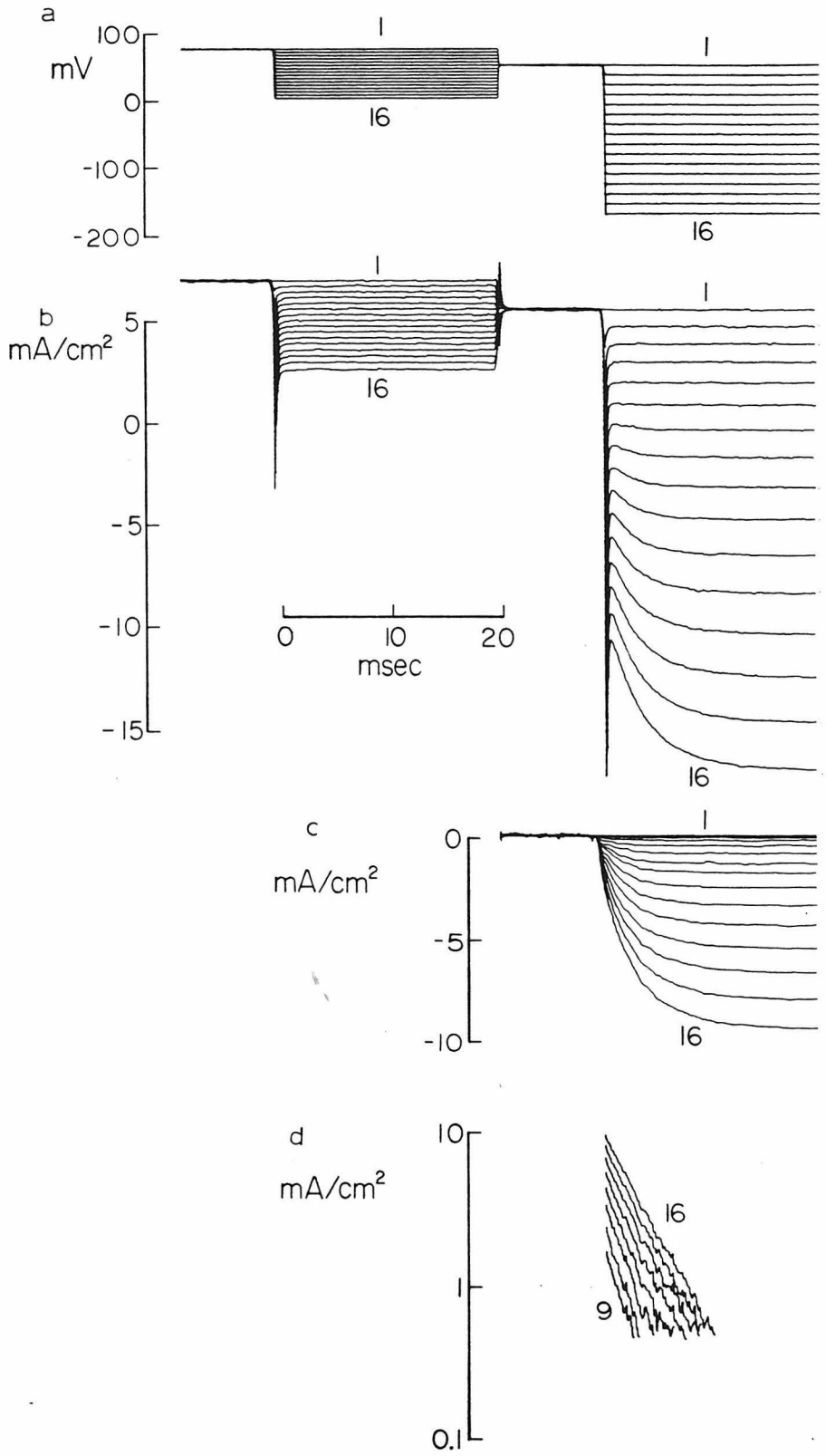
a
100
mV
0
-100
-200
1
16
1
16
b
mA/cm²
5
0
-5
-10
-15
1
16
1
16
0
10
20
msec
c
mA/cm²
0
-5
-10
1
16
d
mA/cm²
10
1
0.1
16
9

33-43

currents associated with electrically excitable sodium conductance as well as agonist-induced current (Armstrong, 1975). These gating currents, due to nonlinear capacitance, are not eliminated by TTX. Thus, the early relaxation currents are distorted by the presence of gating currents.

Measurement of Voltage-Jump Relaxations. Agonist-induced currents relax to steady state along a simple exponential time course (Figures 9c and 10d). Some voltage-jump relaxations could be followed for more than 95% of the approach to steady state. In acetylcholine, voltage-jump relaxations can be described by a single exponential rate constant, $1/\tau$. Such voltage-jump relaxations do not contain any long time constant components. However, a fast component with a decay time constant of 200 μsec or less would be impossible to resolve due to temporal limitations of the voltage-clamp circuit. Therefore, voltage-jump relaxations in acetylcholine could contain a fast decay component with a rate at least five times the observed decay rate. Such a condition is typical of relaxations between only two chemical states or of relaxations involving a rate-limiting step. Like Electrophorus electroplaques, amphibian skeletal muscle fibers have agonist-induced currents which relax with a single exponential rate constant (Adams, 1975c; Neher and Sakmann, 1975; Adams, 1977). In receptor-rich fragments of Torpedo electric organ, relaxations have been measured using intrinsic fluorescence of the receptor (Bonner et al., 1976) and quinacrine-induced fluorescence (Grunhagen et al., 1976). In both cases, a fast, simple exponential relaxation was

Figure 11. Evidence that voltage-jump relaxation rates depend instantaneously on membrane voltage. Carbachol, 100 μM. Insert: superimposed voltage traces. V_1 = +50 mV; V_3 = -235 mV. V_2 lasted 7.5 msec. Open circles: relaxation rates for the jump from V_1 to V_2. Filled circles: relaxation rates for the jump from V_2 to V_3. 95% confidence limits are shown. Temperature, 15°.

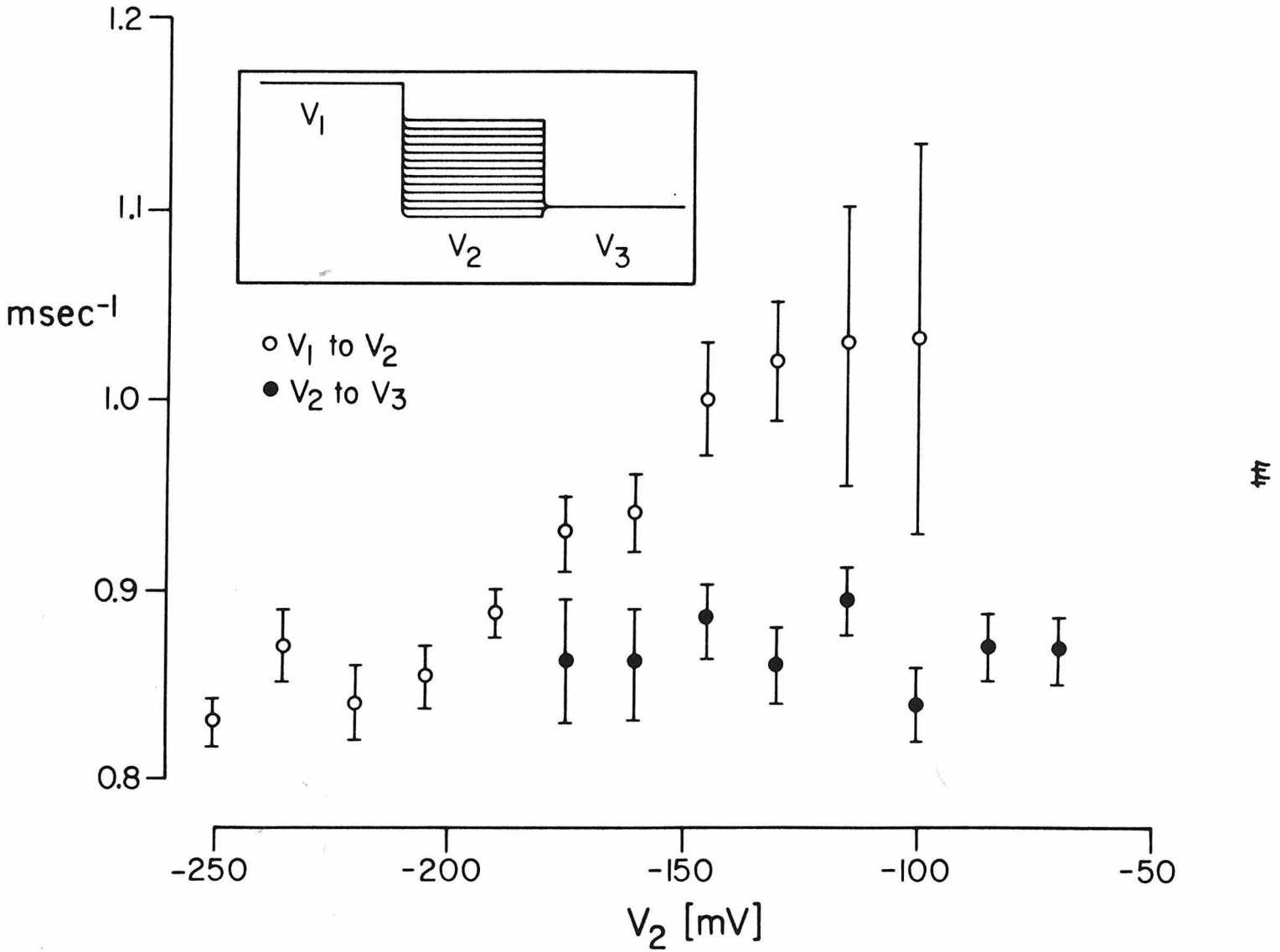
1.2
1.1
1.0
0.9
0.8
msec⁻¹
V1
V2
V3
o V1 to V2
● V2 to V3
-250
-200
-150
-100
-50
V2 [mV]

associated with receptor activation.

Voltage Dependence of Relaxation Rates. Voltage-jump relaxation rates depend on the membrane voltage after the voltage jump. For the data of Figure 11, an electroplaque was exposed to the cholinergic agonist carbachol. The innervated membrane was clamped to the indicated series of voltages and the resulting relaxation rates were measured. For the jump from the fixed voltage V_1 to the variable voltage V_2, relaxation rates changed systematically with V_2. However, for the jump from the variable voltage V_2 to the fixed voltage V_3, relaxation rates were constant. Thus, voltage-jump relaxation rates depend on the membrane voltage after the jump and not on the membrane voltage before the jump. Similarly, relaxation rates are the same for voltage jumps from +50 to -100 mV (an "on" type jump) and for voltage jumps from -175 to -100 mV (an "off" type jump). Both on and off type voltage-jump relaxations depend on the membrane voltage after the voltage jump, regardless of the nature of the agonist or its concentration (Table I). All of these experiments show that voltage-jump relaxation rates do not depend on the previous history of the membrane voltage. Such an instantaneous voltage dependence is a necessary condition for the equivalence of voltage-jump relaxation rates and rates of spontaneous fluctuation in agonist-induced conductance. In amphibian skeletal muscle, voltage-jump relaxations and spontaneous fluctuations have equal rate constants (Naher and Sakmann, 1975).

Voltage-jump relaxation rates increase as the voltage after the jump becomes more positive. The voltage-jump relaxation rate, $1/\tau$,

TABLE I

COMPARISON OF "ON" AND "OFF" RELAXATIONS

Cell	Agonist	$1/\tau$ OFF ($msec^{-1}$)	$1/\tau$ ON ($msec^{-1}$)
20-32	ACh, 55 μM	0.25 ± .02	0.24 ± .02
	Carb, 50 μM	0.42 ± .03	0.39 ± .04
20-41	ACh, 75 μM	0.43 ± .03	0.43 ± .01
20-51	ACh, 75 μM	0.38 ± .03	0.35 ± .03
	Carb, 50 μM	0.61 ± .05	0.63 ± .05
26-61	Sub, 3 μM	0.12 ± .01	0.12 ± .01
	Sub, 5 μM	0.20 ± .02	0.19 ± .01

Rate constants for voltage-jump relaxations to a final voltage of -100 mV. Starting voltage was +50 mV for "on" jumps and -175 mV for "off" jumps. SEM of each observation is given. Temperature, 9°.

Figure 12. Comparison of voltage-jump relaxation rates with PSC decay rates. Linear plots of rate constants vs. membrane voltage. Open circles: voltage-jump relaxation rates in 10 μM acetylcholine. Filled circles: averaged PSC decay rates from five electroplaques. Error bars indicate ± 2 SEM. The smooth curve through the PSC data is an exponential fit to the data using equation (2). The smooth curve through the voltage-jump data is the same exponential plus a constant (see text). Temperature, 15°.

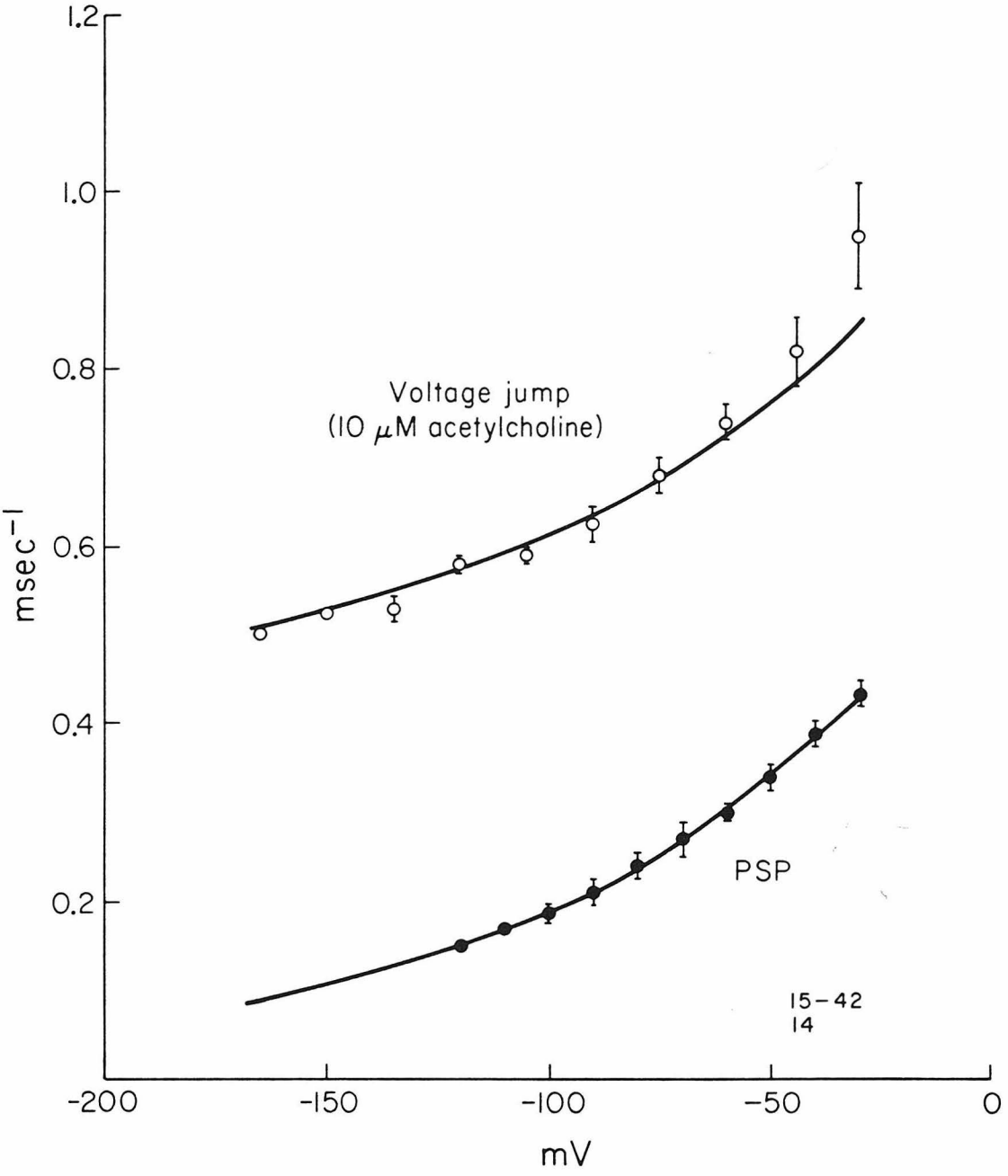
1.2
1.0
0.8
0.6
0.4
0.2
msec⁻¹
Voltage jump
(10 μM acetylcholine)
PSP
15-42
14
-200
-150
-100
-50
0
mV

is greater than the corresponding PSC decay rate, α, at all voltages. Voltage-jump relaxation rates in acetylcholine can be described by an equation similar to that for the PSC decay rate:

$$1/\tau = C + \alpha_0 \exp(V/V_1) \qquad (3)$$

where C is a voltage-independent constant (Figure 12). Experimentally, V_1 equals 82 ± 10 mV (mean ± SD, 5 cells) at 15°, which is essentially equal to the value of V_1 in equation (2) for the PSC decay rate. With the notable exception of the constant C in equation (3), similar results are obtained in amphibian skeletal muscle fibers for voltage-jump relaxations (Adams, 1975c, 1977; Neher and Sakmann, 1975) and spontaneous fluctuations (Katz and Miledi, 1972; Anderson and Stevens, 1973; Neher and Sakmann, 1975; Colquhoun et al., 1977).

Agonist Concentration and Relaxation Rates. For a given agonist, the term C in equation (3) increases with increasing agonist concentration. The concentration dependence of C does not change with membrane voltage (Figure 13). In Electrophorus electroplaques, signal-to-noise limitations prevent measurement of voltage-jump relaxations at agonist concentrations below about $0.3K_{app}$ for the equilibrium dose vs. conductance relation. Desensitization prevents reliable measurement of agonist-induced currents at agonist concentrations greater than about $5K_{app}$. Within this accessible range of agonist concentrations, voltage-jump relaxation rates increase linearly with agonist concentration (Figure 14a). At -175 mV and 15°, the dose vs. rate relation for voltage-jump relaxations has a slope of 10^7 $M^{-1}sec^{-1}$ when acetylcholine is used as the agonist. Other agonists have different slopes.

Figure 13. Voltage-jump relaxation rates vs. membrane voltage at a number of acetylcholine concentrations. The same curve was fit to all concentrations of acetylcholine. Data from several cells were used. Temperature, 15°.

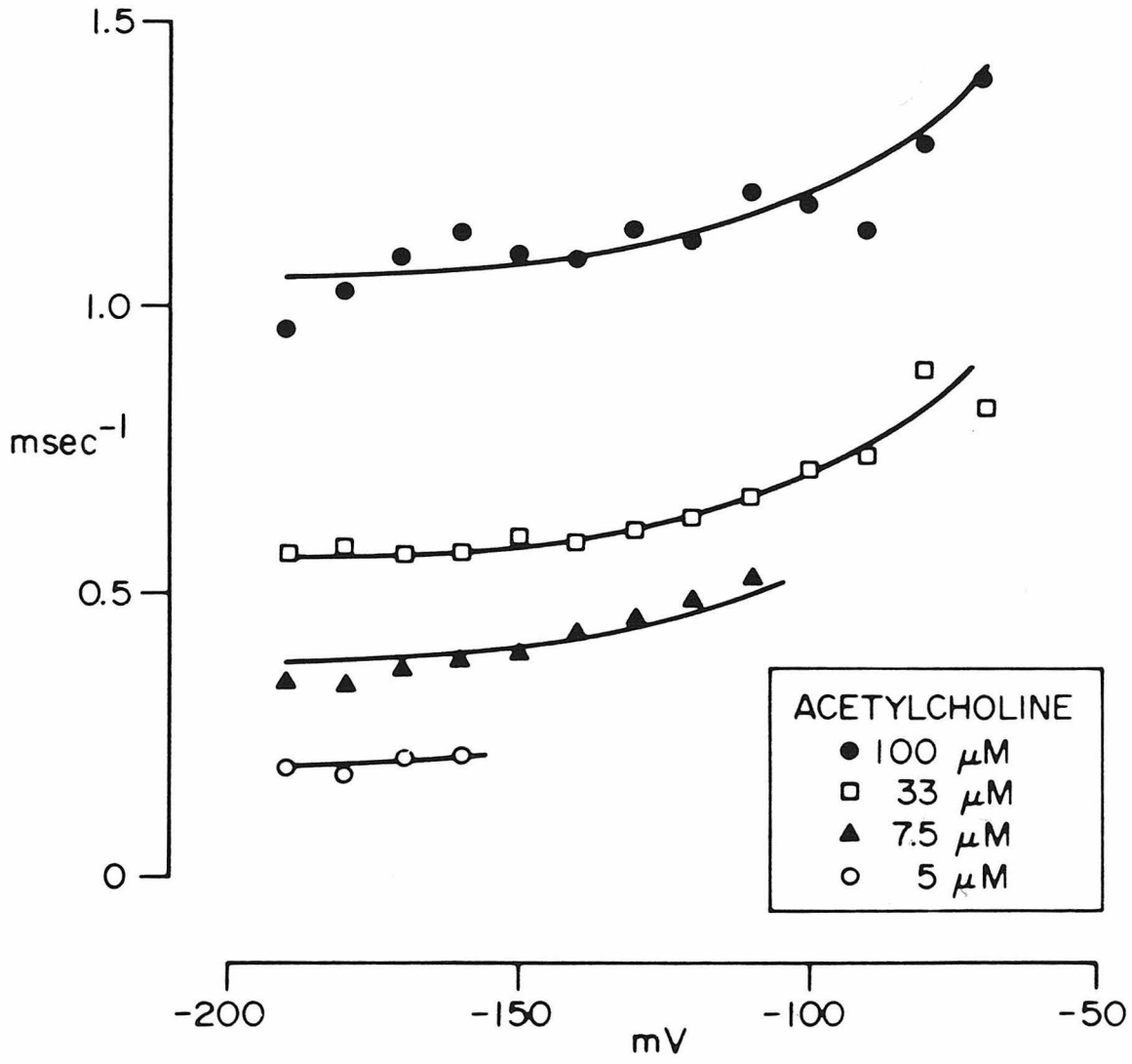
1.5
1.0
0.5
0
msec⁻¹
-200
-150
-100
-50
mV
ACETYLCHOLINE
100 μM
33 μM
7.5 μM
5 μM

In receptor-rich fragments of Torpedo electric organ, the fast relaxation rates associated with receptor activation also increase linearly with agonist concentration, with a slope of 10^6 to 10^7 $M^{-1}sec^{-1}$ for acetylcholine (Bonner et al., 1976; Grunhagen et al., 1976; Neumann and Chang, 1976).

Voltage-jump relaxation rates extrapolate to a nonzero value at zero agonist concentration. As predicted by equations (2) and (3), the extrapolated zero-concentration rate for voltage jumps in acetylcholine equals the PSC decay rate to within experimental error (<20%). Therefore, in equation (3) the term C is equal to zero at zero agonist concentration. Similarly, α_0 is independent of membrane voltage and agonist concentration, although α_0 does depend on the nature of the agonist (Sheridan and Lester, 1975, 1977). In amphibian skeletal muscle, however, voltage-jump relaxation rates and spontaneous fluctuation rates are insensitive to agonist concentration (Adams, 1977) and equal the PSC decay rate when the agonist is acetylcholine (Anderson and Stevens, 1973; Colquhoun et al., 1977).

Voltage-jump relaxation rates increase linearly with agonist concentration through the range of agonist concentrations where the dose vs. conductance relation is demonstrably nonlinear (Figure 14). At any given voltage, the dose vs. current relation is sigmoid, with only a narrow range of agonist concentrations where a linear approximation is valid. The dose vs. rate relation is linear not only in this narrow range but also at higher agonist concentrations where the equilibrium current increases less than linearly with agonist concentration. In Electrophorus electricus, voltage-jump relaxations

Figure 14. Equipotential dose vs. response relations for one electroplaque at -175 mV. (a) Voltage-jump relaxation rate vs. acetylcholine concentration. Arrow indicates the PSC decay rate at the same voltage. (b) Equilibrium agonist-induced current vs. acetylcholine concentration. Filled circles: first concentration series. Open circles: second concentration series. Temperature, 15°.

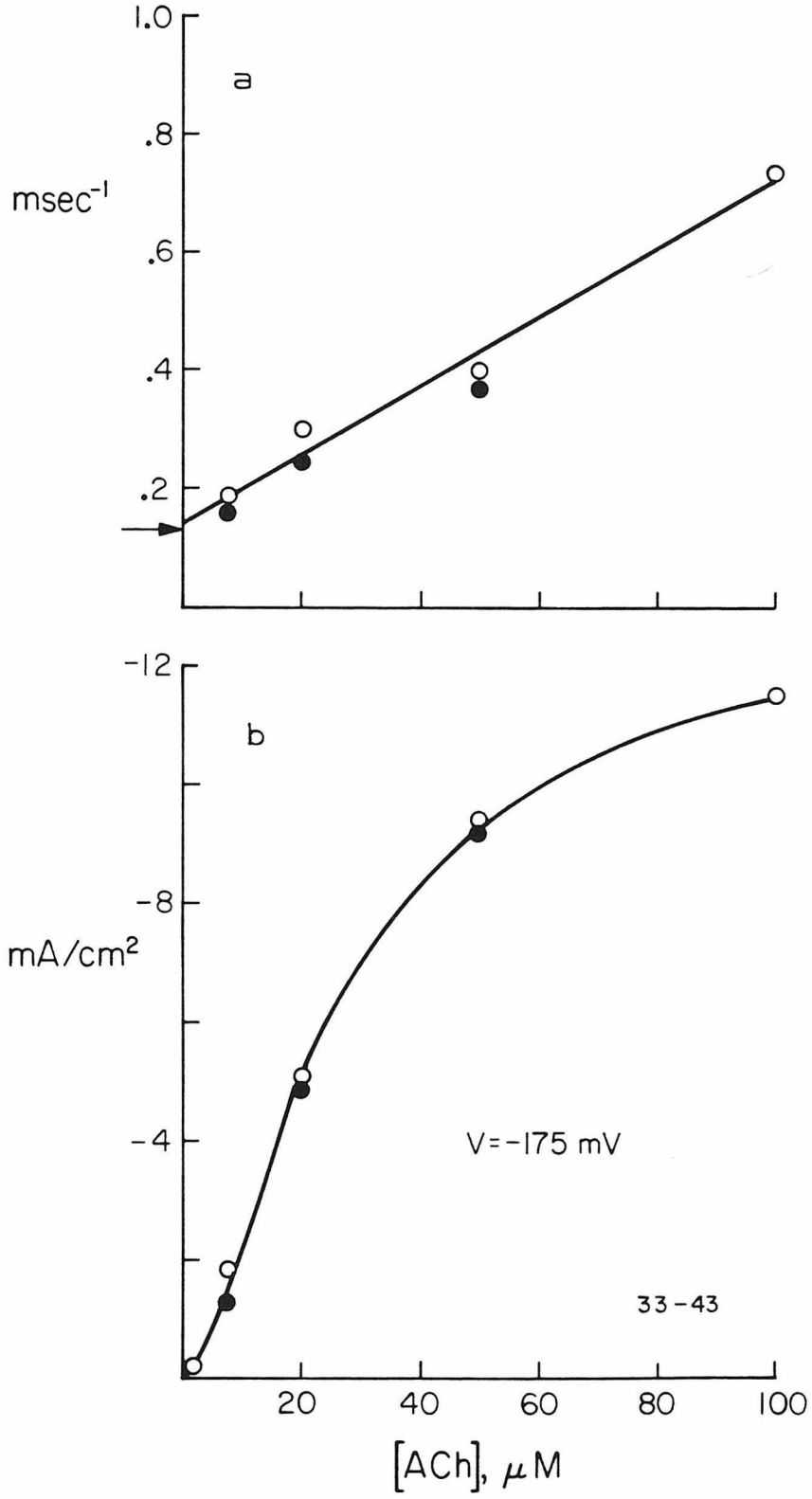
1.0
.8
.6
.4
.2
msec⁻¹
a
-12
-8
-4
mA/cm²
b
V=-175 mV
33-43
20
40
60
80
100
[ACh], μM

cannot be measured at the low agonist concentrations where equilibrium current increases more than linearly with agonist concentration. Thus, although little can be concluded about the dose vs. rate curve at the low concentration extreme, it is clear that the dose vs. rate curve is linear at agonist concentrations where the equilibrium, dose vs. current curve cannot be approximated by a linear relationship. This difference in concentration dependence will be useful in evaluating hypothetical reaction mechanisms.

In Electrophorus electroplaques, α-bungarotoxin irreversibly blocks agonist-induced conductance (Changeux et al., 1970; Lester et al., 1975; Sheridan and Lester, 1975, 1977). The extent of this blockade depends on the toxin concentration and the duration of exposure. Thus, α-bungarotoxin can block a portion of the nicotinic receptor population, leaving the rest of the nicotinic receptors functional. Such an α-bungarotoxin treatment reduces agonist-induced current but does not affect voltage-jump relaxation rates (Figure 15). These results support the assumption that the agonist-receptor reaction is independent of receptor "concentration" because the agonist concentration is rapidly buffered near the receptors by diffusion from the bulk solution (pool A). These results also show that voltage-jump relaxation rates are independent of the agonist-induced conductance.

Figure 15. Effects of α-bungarotoxin on electroplaque responses in 30 μM carbachol. (a) Linear plot of voltage-jump relaxation rate vs. membrane voltage. (b) Equilibrium agonist-induced current vs. membrane voltage. Filled circles: control responses. Open circles: responses after treatment with 5×10^{-8} M α-bungarotoxin for 15 min. Error bars indicate ± SEM for rate measurements. Temperature, 15°.

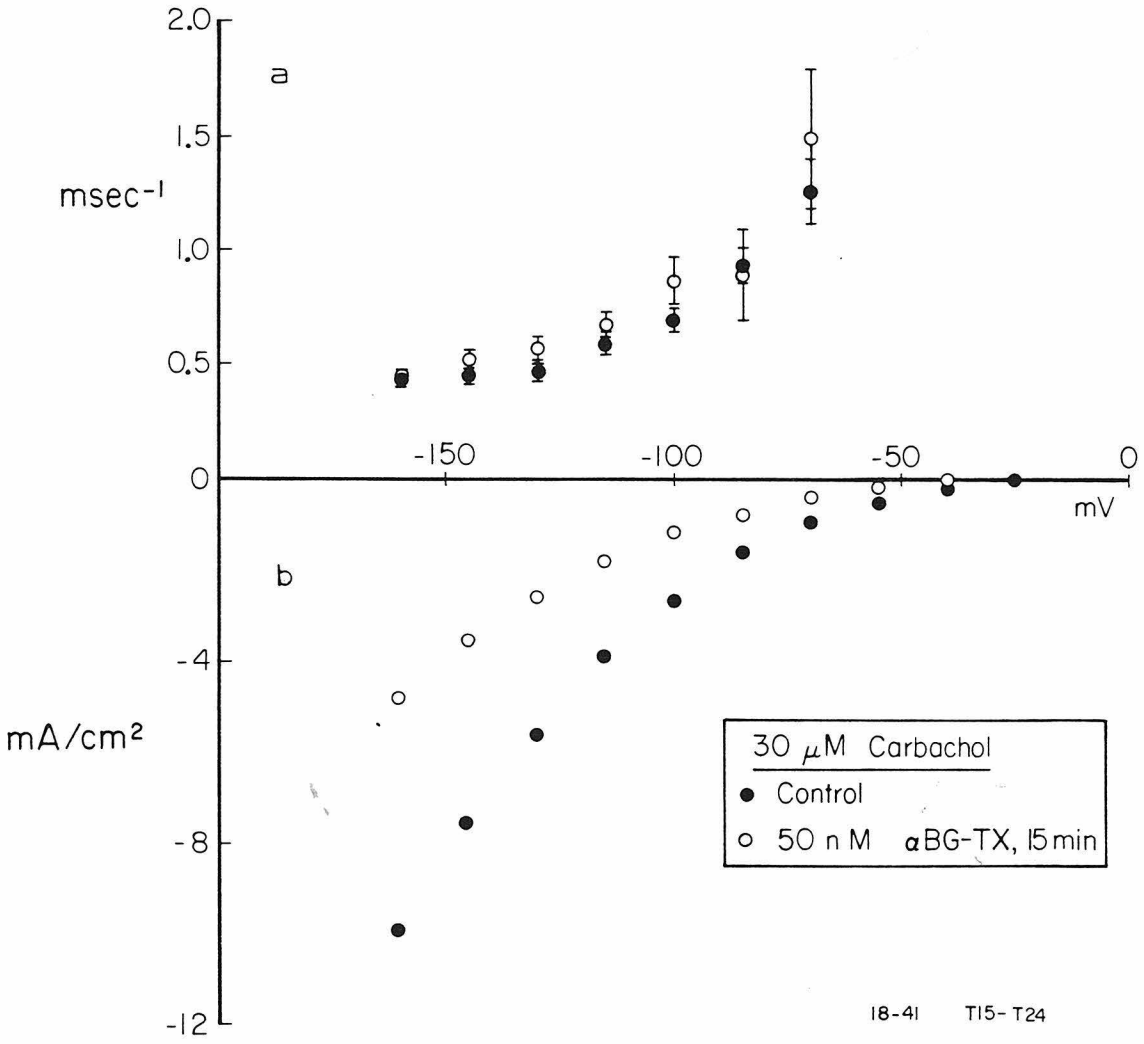
2.0
1.5
1.0
0.5
0
msec⁻¹
a
-150
-100
-50
0
mV
b
-4
-8
-12
mA/cm²
30 μM Carbachol
Control
50 n M αBG-TX, 15 min
18-41 T15-T24

THEORETICAL RELATIONS BETWEEN KINETICS AND EQUILIBRIA

Restrictions Imposed on Kinetic Models. Experimental kinetic and equilibria data impose criteria for kinetic models. For the nicotinic receptor, these criteria fall into three general categories. First, at equilibrium, the dose vs. conductance relation must have a sigmoid form similar to equation (1). Also, the apparent dissociation constant (or agonist concentration at half-maximal conductance) must increase exponentially as membrane voltage becomes more positive. Second, voltage-jump relaxations must follow a simple exponential time course, even when relaxation amplitudes are a significant fraction of the maximum agonist-induced conductance. Third, voltage-jump relaxation rates must increase linearly with agonist concentrations from about $0.3K_{app}$ to $5K_{app}$. Furthermore, at zero agonist concentration, the voltage-jump relaxation rate in acetylcholine must extrapolate to the PSC decay rate for the same voltage. In turn, the PSC decay rate increases exponentially as membrane voltage becomes more positive.

Many kinetic models could satisfy these experimentally imposed criteria. However, one further restriction can be placed on any kinetic model of the nicotinic receptor. A nicotinic receptor can assume only two conductances. One conductance level is zero (the "closed" state) and the other has a conductance of γ (the "open" state). Graded agonist-induced conductance implies that a variable fraction of the receptor population assumes the open state and not that the conductance of each receptor is continuously variable. Thus, voltage-jump relaxations and PSC's are changes in the distribution of the receptor population between open and closed states. Such a

two-state model is supported in amphibian skeletal muscle by spontaneous fluctuations and single-channel recordings which reveal a unique conducting state of the nicotinic receptor with a chord conductance of about 10^{-11}mho (Katz and Miledi, 1972; Anderson and Stevens, 1973; Neher and Sakmann, 1976; Colquhoun et al., 1977; Dionne and Ruff, 1977; but see also Colquhoun et al., 1975). Similar data are not available for Electrophorus electroplaques.

Single Bimolecular Association Models. One simple, kinetic model assumes a single bimolecular association of agonist and receptor followed by a conformational change to the receptor's conducting state. The reaction pathway is:

$$A + R \underset{k_{-1}}{\overset{k_{+1}}{\rightleftharpoons}} AR \underset{k_{-c}}{\overset{k_{+c}}{\rightleftharpoons}} AR^{*} \qquad (4)$$

where A is agonist, R is receptor, AR is a closed intermediate, and AR^{*} is the open form of the receptor. The rate constants $k_{\pm 1}$ refer to the binding reaction, and the rate constants $k_{\pm c}$ refer to the conformational change. If either conformational change or binding is rate limiting, then voltage-jump relaxations are simple exponentials.

If conformational change is rate limiting, then voltage-jump relaxations are simple exponentials with a voltage-jump relaxation rate:

$$1/\tau = k_{+c}\left[\frac{k_{+1}A}{k_{+1}A + k_{-1}}\right] + k_{-c} . \qquad (5)$$

When A equals zero, $1/\tau$ equals k_{-c}. Therefore, the PSC decay rate is k_{-c}, and k_{-c} is the only voltage sensitive rate constant. According to equation (5), voltage-jump relaxation rates should increase with agonist

concentration. However, the increase is hyperbolic, not linear, with a half-maximal point at k_{-1}/k_{+1} and a zero-concentration intercept of k_{-c}. For agonist concentrations less than k_{-1}/k_{+1}, voltage-jump relaxation rates increase nearly linearly with agonist concentration.

If binding is rate limiting, then voltage-jump relaxations are simple exponentials because the binding step is pseudo-first-order. In equation (4), binding should depend on both the agonist concentration and the number of functional receptors per unit area of membrane. From the experimental results with α-bungarotoxin, it can be shown that relaxation rates do not depend on the number of functional receptors. This apparently first-order behavior is probably due to rapid buffering of agonist concentrations near the receptors by diffusion from the bulk solution. Under these conditions, the voltage-jump relaxation rate is:

$$1/\tau = k_{+1}A + k_{-1}k_{-c}/(k_{+c} + k_{-c}). \qquad (6)$$

Equation (6) predicts that voltage-jump relaxation rates increase linearly with agonist concentration. At zero agonist concentration, the relaxation rate equals $k_{-1}k_{-c}/(k_{+c} + k_{-c})$, which is the PSC decay rate. This PSC decay rate is voltage dependent when either k_{-1}, k_{-c} or k_{+c} is voltage sensitive. Equation (6) then meets all experimental kinetic criteria.

Whichever reaction step is rate limiting, the equilibrium agonist-induced conductance is:

$$g = r\gamma \left[\frac{k_{+c}k_{+1}A}{k_{+c}k_{+1}A + k_{-c}k_{+1}A + k_{-c}k_{-1}} \right] \qquad (7)$$

where r is the receptor population accessible to agonist. Equation (7)

predicts a hyperbolic dose vs. conductance relation with a half-maximal conductance at $k_{-1}k_{-c}/k_{+1}(k_{+c} - k_{-c})$. However, the dose vs. conductance relation is actually sigmoid. Therefore, the single bimolecular association model, equation (4), fails to meet the experimentally established criteria for equilibrium conductance.

Voltage Sensitive Conformational Change. It is useful to consider the limitations of conformational change independently of any specific model for the nicotinic receptor. If conformational change is voltage sensitive and not rate limiting, the ratio $k_{+c}/(k_{+c} + k_{-c})$ determines the voltage dependence of instantaneous, agonist-induced conductance. Instantaneous, agonist-induced conductance was not found to be voltage dependent at voltages more negative than -30 mV (Figure 2). Therefore, for conformational change to be voltage sensitive and not be rate limiting, the ratio $k_{+c}/(k_{+c} + k_{-c})$ must nearly equal one at voltages more negative than -30 mV.

If conformational change is rate limiting and voltage sensitive, then equation (5) implies that $(k_{+c} + k_{-c})$ must exceed the fastest observed voltage-jump relaxation rate (about 2 $msec^{-1}$ at 15°). Also, for relaxation rates to increase linearly with the observed agonist concentrations, the half-maximal point of the dose vs. rate relation must be at least five times the observed K_{app} for agonist-induced conductance. Considering the specific case posed by equations (5) and (7), the ratio k_{-1}/k_{+1} must exceed K_{app}, $k_{-1}k_{-c}/k_{+1}(k_{+c} - k_{-c})$, by at least five-fold. This implies that the ratio $(k_{+c} - k_{-c})/k_{-c}$ must be greater than five.

All of these limitations, taken togeather, indicate that if conformational change is voltage sensitive, the open conformation is favored at all voltages more negative than -30 mV.

Dimerization Models. Voltage-sensitive dimerization regulates the gramicidin-induced conductance in artificial membranes (Bamberg and Lauger, 1973; Zingsheim and Neher, 1974). A similar model for the nicotinic receptor is:

$$2A + 2R \underset{k_{-1}}{\overset{k_{+1}}{\rightleftharpoons}} 2AR \underset{k_{-d}}{\overset{k_{+d}}{\rightleftharpoons}} (AR)_2 \qquad (8)$$

where $(AR)_2$ is the open receptor configuration with a conductance of γ and where the rate constants $k_{\pm d}$ refer to the voltage-dependent dimerization. At equilibrium:

$$k_{+d} \left[(r - 2(AR)_2)(k_{+1}A/(k_{+1}A + k_{-1}))\right]^2 = k_{-d} (AR)_2 . \qquad (9)$$

Equation (9) predicts a sigmoid dose vs. conductance relation with a half-maximal conductance:

$$K_{app} = k_{-1}/k_{+1} \left[(r - p)(2k_{+d}/pk_{-d})^{\frac{1}{2}} - 1\right] \qquad (10)$$

where:

$$p = r/2 + k_{-d}/8k_{+d} - (8rk_{-d}/k_{+d} + (k_{-d}/k_{+d})^2)^{\frac{1}{2}}/8. \qquad (11)$$

Thus, K_{app} is a function of the voltage-sensitive dimerization rate constant(s). However, it should be noted that K_{app} also depends on the receptor population, r, and might be expected to change in response to noncompetitive antagonists. For this dimerization model, it may be advisable to redefine a receptor population as an interacting subset of receptors in the postsynaptic membrane. If the postsynaptic membrane contains a large number of such subsets, each having a small number of

receptors, then antagonists could block postsynaptic receptors in units of one subset, r, and still not change K_{app}.

Relaxation kinetics are somewhat complicated in the dimerization model. If dimerization is rate limiting, voltage-jump relaxations are simple exponentials when rk_{+d}/k_{-d} is less than about three (Bamberg and Lauger, 1973). With this restriction, voltage-jump relaxation rates are:

$$1/\tau = k_{-d} + k_{+d}\left[k_{+1}A/(k_{+1}A + k_{-1})\right]\left[-s + (s(s + 8r))^{\frac{1}{2}}\right] \quad (12)$$

where:

$$s = (k_{-d}/k_{+d})((k_{-1} + k_{+1}A)/k_{+1}A)^2. \quad (13)$$

Equation (12) predicts that when A equals zero, $1/\tau$ equals k_{-d}. Therefore, k_{-d} is the PSC decay rate and the data suggest that it is the only voltage sensitive rate constant. Equations (12) and (13) also predict that voltage-jump relaxation rates increase with agonist concentration. The increase is essentially hyperbolic with a half-maximal point close to K_{app} for the dose vs. conductance relation, given by equations (10) and (11). Both the dose vs. rate curve and the dose vs. conductance curve level off at the same agonist concentrations. Therefore, the rate-limiting dimerization model does not satisfy the experimental kinetic data.

If binding is rate limiting, "on" type voltage-jump relaxations differ markedly from a simple exponential under all conditions. Therefore, the dimerization model, equation (8), fails to meet experimental relaxation kinetics criteria.

Concerted Transition Models. The Monod, Wyman, and Changeux model for

receptors, then antagonists could block postsynaptic receptors in units of one subset, r, and still not change K_{app}.

Relaxation kinetics are somewhat complicated in the dimerization model. If dimerization is rate limiting, voltage-jump relaxations are simple exponentials when rk_{+d}/k_{-d} is less than about three (Bamberg and Lauger, 1973). With this restriction, voltage-jump relaxation rates are:

$$1/\tau = k_{-d} + k_{+d}\left[k_{+1}A/(k_{+1}A + k_{-1})\right]\left[-s + (s(s + 8r))^{\frac{1}{2}}\right] \quad (12)$$

where:

$$s = (k_{-d}/k_{+d})((k_{-1} + k_{+1}A)/k_{+1}A)^2. \quad (13)$$

Equation (12) predicts that when A equals zero, $1/\tau$ equals k_{-d}. Therefore, k_{-d} is the PSC decay rate and the data suggest that it is the only voltage sensitive rate constant. Equations (12) and (13) also predict that voltage-jump relaxation rates increase with agonist concentration. The increase is essentially hyperbolic with a half-maximal point close to K_{app} for the dose vs. conductance relation, given by equations (10) and (11). Both the dose vs. rate curve and the dose vs. conductance curve level off at the same agonist concentrations. Therefore, the rate-limiting dimerization model does not satisfy the experimental kinetic data.

If binding is rate limiting, "on" type voltage-jump relaxations differ markedly from a simple exponential under all conditions. Therefore, the dimerization model, equation (8), fails to meet experimental relaxation kinetics criteria.

Concerted Transition Models. The Monod, Wyman, and Changeux model for

allosteric enzymes is based on concerted transition of all protomers in the enzyme between inactive and active conformations (Kirschner, 1971; Hammes and Wu, 1974). For the nicotinic receptor such a model is:

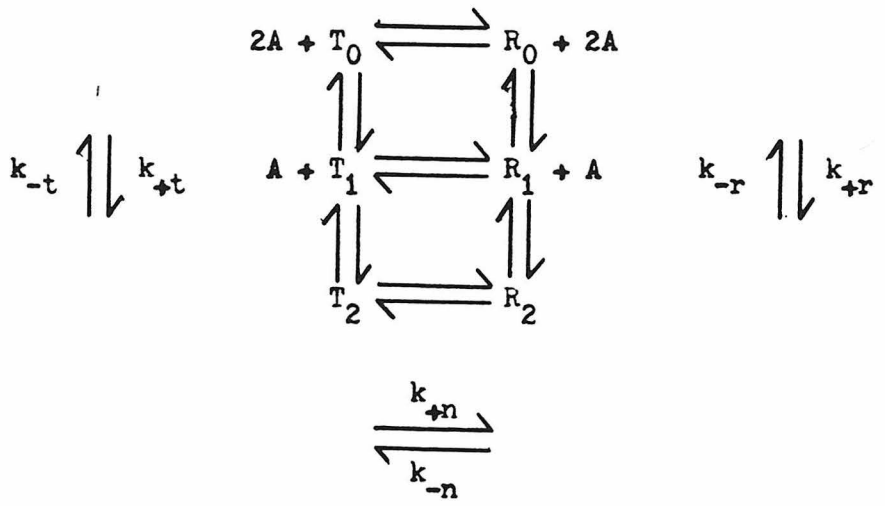

(14)

where T_n is the closed receptor conformation and R_n is the open receptor conformation with a unit conductance γ. This model could have more than the two binding steps shown, but n = 2 is the minimum condition for a Hill coefficient of two (Karlin, 1967a). If all the reaction steps in equation (14) were independent, voltage-jump relaxations could consist of up to seven components. This complexity can be reduced by employing three simple assumptions (Kirschner et al., 1970; Kirschner, 1971; Hammes and Wu, 1974). First, agonist binding to all T_n occurs with the same specific rate constants, $k_{\pm t}$. Second, agonist binding to all R_n occurs with the same specific rate constants, $k_{\pm r}$. Third, either all k_{-n} equal k_{-o} or all k_{+n} equal k_{+o}. If all k_{-n} equal k_{-o}, the principle of microscopic reversibility requires that $k_{+n} = p^n k_{+o}$ where $p = k_{-r}k_{+t}/k_{+r}k_{-t} = K_R/K_T$. Similarly, if all k_{+n} equal k_{+o}, then $k_{-n} = p^n k_{-o}$.

For this simplified form of equation (14), equilibrium agonist-induced conductance is:

$$g = \frac{r\gamma}{1 + (k_{-o}/k_{+o})\left[\frac{1 + pA/K_R}{1 + A/K_R}\right]^2} \qquad (15)$$

where K_R equals k_{-r}/k_{+r}, K_T equals k_{-t}/k_{+t}, and p equals K_R/K_T (Karlin, 1967a). In the absence of agonist, receptor mediated conductance is very small, implying that $k_{-o}/k_{+o} \gg 1$. For $p \ll 1$, the dose vs. conductance relation is sigmoid.

If conformational change is rate limiting, voltage-jump relaxations are simple exponentials. Within the limitations already mentioned, voltage-jump relaxation rates increase with agonist concentration only if all k_{-n} equal k_{-o} and $k_{+n} = p^n k_{+o}$. Under these conditions, the voltage-jump relaxation rate is:

$$1/\tau = k_{-o} + k_{+o}\left[\frac{1 + A/K_R}{1 + pA/K_R}\right]^2 \qquad (16)$$

(Kirschner et al., 1966, Kirschner, 1971; Hammes and Wu, 1974). At zero agonist concentration, equation (16) predicts that $1/\tau$ equals $(k_{-o} + k_{+o})$. Therefore, the sum $k_{-o} + k_{+o}$ is the PSC decay rate and must increase exponentially as membrane voltage becomes more positive. Equation (16) also predicts that voltage-jump relaxation rates increase sigmoidally with agonist concentration. According to equations (15) and (16), both $1/\tau$ and g have nearly identical dose vs. response relations. Since the dose vs. rate relation is actually linear at agonist concentrations where the dose vs. conductance relation is nonlinear (Figure 14), the Monod, Wyman, and Changeux model with rate-limiting concerted transitions fails to meet experimental kinetic criteria.

If either agonist binding to the T_n conformations or agonist binding to the R_n conformations is rate limiting, voltage-jump relaxations cannot be simple exponentials. Therefore, the concerted transition model, equation (14), does not account for the observed nicotinic receptor relaxation kinetics.

Sequential Binding Models. The Adair, Koshland, Nemethy, and Filmer model for allosteric enzymes is based on sequential binding reactions, each of which is followed by a conformational change (Koshland et al., 1966; Koshland and Neet, 1968; Hammes and Wu, 1974). If conformational change is closely coupled to binding, each sequential binding and conformational change is kinetically equivalent to a binding step alone. For the nicotinic receptor, such a sequential binding model is:

$$2A + R \underset{k_{-1}}{\overset{2k_{+1}}{\rightleftharpoons}} A + AR \underset{2k_{-2}}{\overset{k_{+2}}{\rightleftharpoons}} A_2R \qquad (17)$$

where A_2R is the open receptor conformation with a conductance of γ. According to this model, each receptor has two binding sites for agonist. These binding sites are assumed to be equivalent before any agonist is bound and after two agonist molecules are bound, resulting in the statistical factors of two associated with k_{+1} and k_{-2}. The first binding step cannot be rate limiting. If it were, then the PSC decay rate would equal $2k_{-2}$ and would be too fast to measure. Therefore, the second binding step must be rate limiting in this model.

If the second binding step is rate limiting and voltage sensitive, then voltage-jump relaxations are simple exponentials with a rate constant of:

$$1/\tau = \frac{k_{+2}A^2}{A + k_{-1}/2k_{+1}} + 2k_{-2}. \qquad (18)$$

According to equation (18), when A equals zero, $1/\tau$ equals $2k_{-2}$. Thus, $2k_{-2}$ is the PSC decay rate and must be the only voltage sensitive rate constant. Equation (18) also predicts that voltage-jump relaxation rates increase linearly with agonist concentrations greater than about $0.5\ k_{-1}/k_{+1}$ (Figure 16a). Experimentally, voltage-jump relaxation rates could not be measured at agonist concentrations below about $0.7\ k_{-1}/k_{+1}$; so the predicted dependence is not inconsistent with the observed concentration dependence. When k_{-2} is the only voltage sensitive reaction rate, the dose vs. rate relation is independent of voltage. Therefore, equation (18) predicts the observed voltage and agonist concentration dependence of the relaxation rate. Under these same conditions, equilibrium agonist-induced conductance is:

$$g = r\gamma \left[\frac{A^2}{A^2 + 2Ak_{-2}/k_{+2} + k_{-1}k_{-2}/k_{+1}k_{+2}} \right]. \qquad (19)$$

Equation (19) predicts a sigmoid dose vs. conductance relation equivalent to equation (1) if k_{-1}/k_{+1} approximately equals k_{-2}/k_{+2} (Figure 16b). In equation (19), half-maximal conductance occurs at:

$$K_{app} = \left[k_{-2}k_{+1} + (k_{-2}k_{+1}(k_{-2}k_{+1} + k_{+2}k_{-1}))^{\frac{1}{2}} \right] / k_{+1}k_{+2}. \qquad (20)$$

Since the PSC decay rate equals $2k_{-2}$, both rates must increase e-fold with every +87 mV change in membrane voltage. If k_{-2} is the only voltage sensitive rate constant in the reaction, equation (20) predicts that K_{app} increases nearly e-fold with every +87 mV change in membrane voltage, as was found experimentally (Figure 5). Therefore, equation (19)

Figure 16. Theoretical dose vs. response curves for the sequential binding model at one voltage. (a) Voltage-jump relaxation rate vs. normalized agonist concentration. (The equivalent PSC decay rate equals $2k_{-2}$.) (b) Fractional equilibrium conductance vs. normalized agonist concentration.

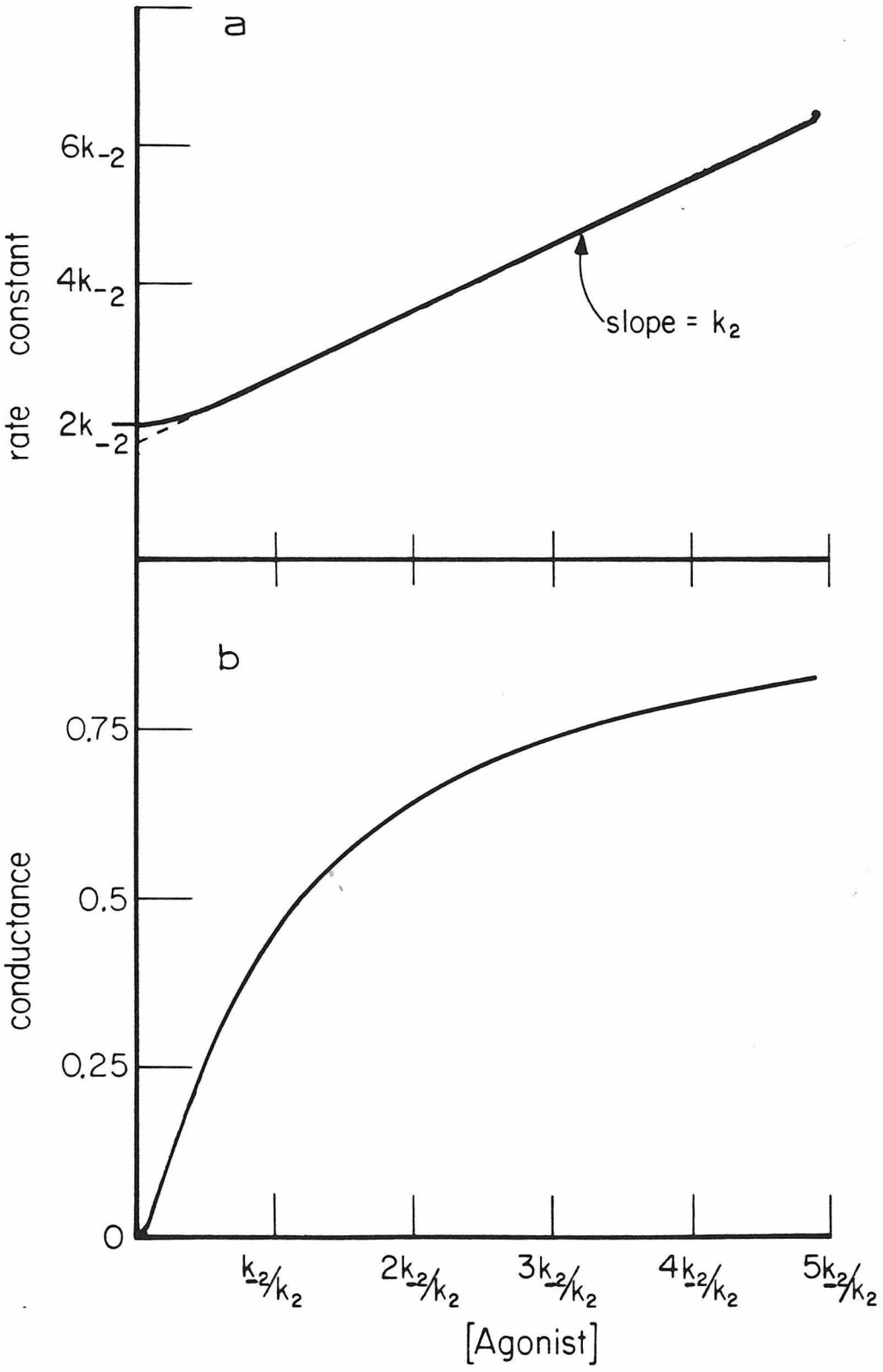
a
6k-2
4k-2
2k-2
rate constant
slope = k2
b
0.75
0.5
0.25
0
conductance
k-2/k2
2k-2/k2
3k-2/k2
4k-2/k2
5k-2/k2
[Agonist]

predicts the voltage and agonist concentration dependence observed in equilibrium agonist-induced conductance. However, because k_{-2} is voltage sensitive, k_{-2}/k_{+2} equals k_{-1}/k_{+1} at only one voltage. Consequently, the predicted dose vs. conductance relation changes shape as a function of voltage. No such effect was observed (Figure 4), but this voltage dependent effect might be obscured by experimental uncertainty in the data.

The ratio k_{-2}/k_{+2} equals the ratio k_{-1}/k_{+1} at all membrane voltages only if both k_{-2} and k_{-1} are voltage sensitive. Under these conditions, the equilibrium agonist-induced conductance is:

$$g = r\gamma \left[\frac{A}{A + k_{-2}/k_{+2}} \right]^2 \qquad (21)$$

with a half-maximal conductance at:

$$K_{app} = (1 + \sqrt{2})\, k_{-2}/k_{+2}. \qquad (22)$$

Again, equation (21) predicts a sigmoid dose vs. conductance relation, and K_{app} has the same voltage dependence as $2k_{-2}$ and the PSC decay rate. Furthermore, the dose vs. conductance relation no longer changes shape as a function of voltage. Assuming that the second binding step is still rate limiting, the voltage-jump relaxation rate is:

$$1/\tau = \frac{(k_{+2}A)^2}{k_{+2}A + k_{-2}/2} + 2k_{-2}. \qquad (23)$$

Equation (23) differs from equation (18) only in that the dose vs. rate relation changes as a function of membrane voltage. Thus, in equation (23) the voltage-jump relaxation rate is not the sum of a voltage insensitive constant and the PSC decay rate as stipulated in equation (3). Specifically, equation (23) predicts a decrease in the voltage

dependence of the relaxation rate. This decrease is greater at higher agonist concentrations but is less than 15% at the highest agonist concentrations tested. Decreases of this magnitude probably would not be detectable in these experiments.

As a final test of the sequential binding model, theoretical curves can be fit to experimental results from Electrophorus electroplaques using as many known parameters as possible. Acetylcholine is the best agonist for this purpose because PSC decay rates equal $2k_{-2}$ only for acetylcholine. The maximum agonist-induced conductance, $r\gamma$, can be estimated from the dose vs. conductance data. The reversal potential, E, is indicated in both the instantaneous current vs. voltage relation and the peak PSC vs. voltage relation. The reaction rate constant k_{+2} is the slope of the dose vs. rate relation for voltage-jump relaxations in acetylcholine. Both membrane voltage and agonist concentration are known. Thus, only k_{-1} and k_{+1} are free parameters. However, if equations (21) and (23) are used, k_{-1} and k_{+1} are fixed by their relation to k_{-2} and k_{+2} respectively. Figure 17 shows the predictions of the sequential binding model with two voltage sensitive binding steps for experimental data from one electroplaque. As can be seen, the sequential binding model adequately accounts for the experimental kinetic and equilibrium data.

The sequential binding model makes several predictions that cannot presently be verified in experiments on Electrophorus electroplaques. First, the voltage-jump relaxation rate is essentially independent of agonist concentrations below about $0.5\ k_{-1}/k_{+1}$. Second, voltage-jump relaxation rates increase linearly with agonist concentration until the

Figure 17. Comparison of theory and data for the sequential binding model with two voltage-sensitive binding steps. Upper panel: voltage-jump relaxation rates vs. membrane voltage. Predicted curves from equation (23). Lower panel: equilibrium agonist-induced current vs. membrane voltage. Predicted curves from equation (21). The maximum agonist-induced current is shown by the dashed line. The reversal potential was estimated to be 0 mV. Acetylcholine concentrations were as indicated. Temperature, 15^{o}.

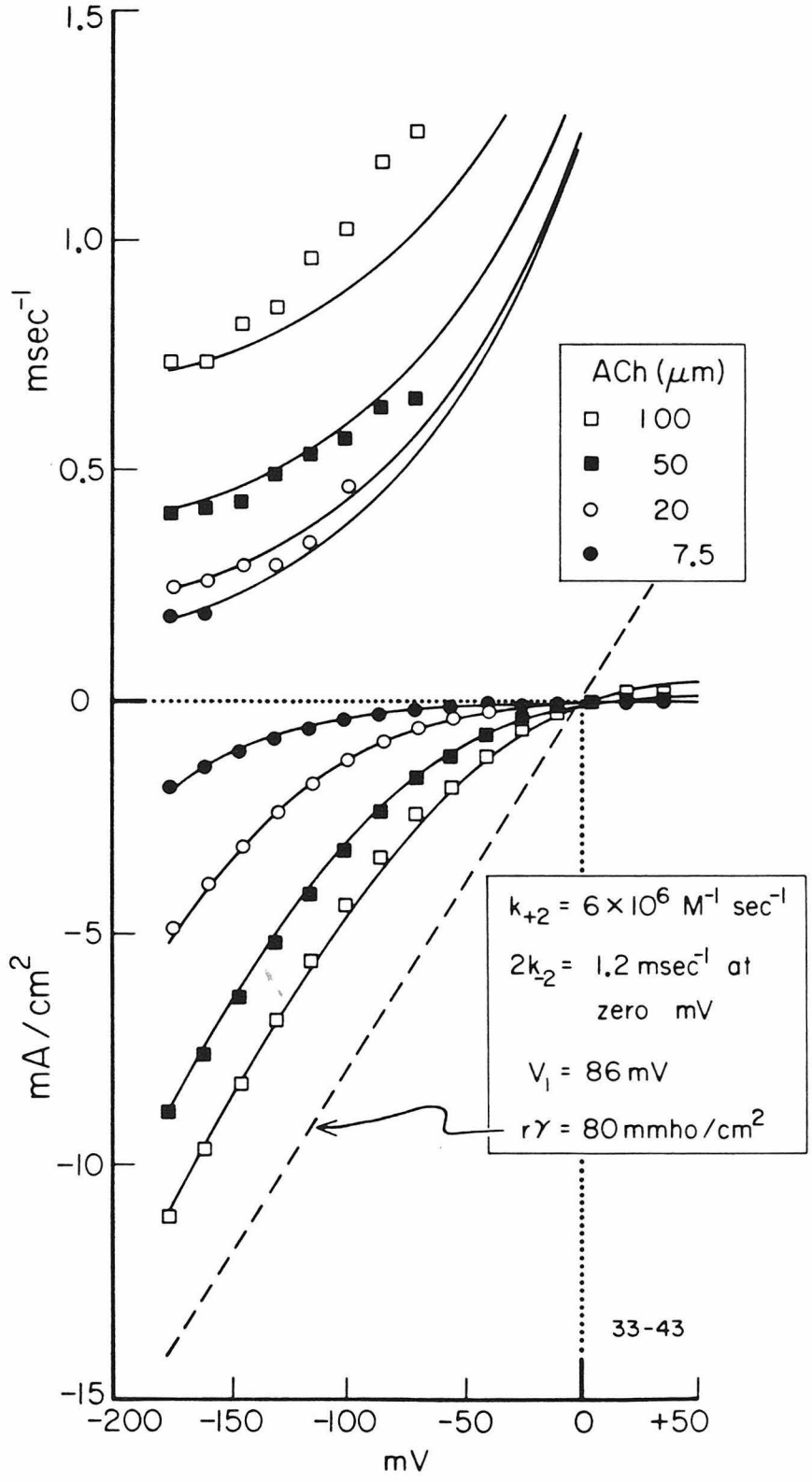
1.5
1.0
0.5
0
-5
-10
-15
msec⁻¹
mA/cm²
-200
-150
-100
-50
0
+50
mV
ACh (μm)
100
50
20
7.5
k+2 = 6 × 10⁶ M⁻¹ sec⁻¹
2k-2 = 1.2 msec⁻¹ at zero mV
V1 = 86 mV
rγ = 80 mmho/cm²
33-43

binding rates approach the rates of other transitions in the reaction, such as conformational change. Third, the first binding step would cause a second relaxation component if this component could be resolved by the voltage-clamp circuit. Fourth, the number of voltage-sensitive binding steps could be determined by observing the voltage dependence of relaxation rates in high agonist concentrations or by better measurements of equilibrium dose vs. conductance relations at different voltages. The verification of these predictions awaits similar measurements on a preparation with better signal-to-noise limitations or a better relaxation method for Electrophorus electroplaques. It should be noted, however, that the first prediction of the sequential binding model would account for the observed lack of agonist concentration effects on relaxation rates in amphibian skeletal muscle, where low agonist concentrations are used.

PART TWO

Studies of Cholinergic Mechanisms in Raia Electroplaques.

MATERIALS AND METHODS

Preparation. Sections of tail, containing the electric organ, were removed from live, adult Raia erinacea and stored in elasmobranch Ringer solution at 8°. Electroplaques in these sections retained normal resting potentials for several days after removal from the animal. Before use, the electric organ was isolated from the section of tail, cleaned of peripheral connective tissue, and mounted in one cm lengths on a Silastic rubber stage. The stage was immersed in a bath containing Ringer solution. The one cm lengths of electric organ contained 20 to 30 electroplaques, each in a connective tissue capsule. Raia erinacea electroplaques are roughly disc shaped, 0.5 to 1.0 mm in diameter and about 50μm thick (Bennett, 1961). Temperature was controlled with a Peltier device beneath the bath.

Solutions. Elasmobranch Ringer solution contained (mM): NaCl, 250; KCl, 4; $CaCl_2$, 5; $MgCl_2$, 2; Urea, 330. This solution was buffered with 5 mM HEPES adjusted to pH 7.4 with NaOH. Drugs were added in Ringer solution without compensation for osmolarity. Bath solutions could be completely changed in less than one minute. At the electroplaque surface, however, solution changes were much slower. Unless otherwise indicated, all drugs were allowed to come to equilibrium effect before data were taken.

Electrical Arrangements. Single electroplaques were impaled with two microelectrodes. The electrodes were filled with 3 M KCl and had resistances of 1 to 5 megohms. One intracellular electrode monitored the membrane voltage and the other electrode passed current into the electroplaque under constant-current or voltage-clamp control. Electrode penetrations were stable for several hours; the electroplaque's input resistance and resting potential did not change over the course of the experiments. Similar results were obtained with 10 to 15 megohm electrodes. Therefore, the low resistance electrodes did not damage the electroplaque membrane. Current injected into the electroplaque was returned through a Ag·AgCl electrode in the bath to a virtual ground circuit which was used to monitor the amount of current injected. Following a jump in clamped membrane voltage, the passive membrane currents settled with a time constant of 200 to 300 μsec. Presynaptic terminals were stimulated with a coaxial electrode near the innervated surface of the electroplaque. During such presynaptic stimulation, voltage clamp of the electroplaque kept the resulting voltage change to less than 5% of the voltage change in an unclamped electroplaque.

NONSYNAPTIC MEMBRANE PROPERTIES

Passive Membrane. Raia electroplaques have resting potentials of -64 ± 9 mV (mean ± SD, 45 cells) at 20°. The effective input resistance, tested with small hyperpolarizing currents, is 15 ± 8 kilohms (mean ± SD, 40 cells)at 20°. At membrane voltages more negative than -50 mV, the electroplaque's current vs. voltage relation is linear (Figure 22).

Space Clamp of Raia Electroplaques. Treating the Raia electroplaque as two discs of membrane bounded at a radius a from the current-passing electrode, the steady-state voltage distribution is:

$$V = \frac{TR_i}{2\pi b} \left[K_1(a/\lambda) I_o(r/\lambda)/I_1(a/\lambda) + K_o(r/\lambda) \right] \qquad (24)$$

where:

$$\lambda = (R_m b/2R_i)^{\frac{1}{2}}. \qquad (25)$$

I_n and K_n are modified Bessel functions of the first and second kinds of order n. T is the current at the origin. V is the membrane voltage at a radial distance r from the origin of the current. The distance between the membrane discs is b. R_m and R_i are the specific membrane and cytoplasm resistances respectively (Jack et al., 1975). For an electroplaque of 0.4 mm radius with $b = 5 \times 10^{-3}$cm, $R_m = 150$ ohm·cm^2, and $R_i = 60$ ohm·cm, the space constant, λ, equals 0.86 mm. Therefore, the radius of the electroplaque, a, is less than $\lambda/2$ for this typical electroplaque. When $a = \lambda/2$, the steady-state voltage varies less than 10% over the cell surface. Thus the passive electroplaque is essentially isopotential when the current-passing electrode is centered in the cell.

For an electroplaque of 0.4 mm radius, 1.5×10^4 ohm input resistance, and with 5×10^{-3}cm between the current-passing and voltage microelectrodes, equation (24) predicts that R_m is 182 ohm·cm^2. Treating the same electroplaque as a spherical cell with equal membrane area, R_m is 150 ohm·cm^2. Since these two values of R_m are nearly equal, the Raia electroplaque is as well described by a spherical cell model as by a planar disc model. Treating the electroplaque as a spherical cell, the passive membrane is isopotential (Cole, 1968).

Delayed Rectification. The Raia electroplaque exhibits delayed rectification at membrane voltages more positive than -50 mV. The delayed rectifier's conductance increases for 10 to 20 msec to a steady-state conductance 10 to 15 times the passive membrane's conductance. The steady-state current due to delayed rectification is outward at all voltages.

When delayed rectification is active, the Raia electroplaque cannot be reliably voltage-clamped. For example, in the typical cell discussed above, delayed rectification reduces the space constant, λ, from 0.86 mm to 0.20 mm. Under these conditions, the electroplaque's radius, 0.4 mm, now equals 2 λ and the steady-state voltage varies by 50% over the electroplaque surface. This is probably the basis of reports that Raia electroplaques are not space clamped when delayed rectification is active (Hille et al., 1965). In Raia electroplaques, the delayed rectifier is not a simple K^+ conductance (Hille et al., 1965; Harris et al., 1976). Neither the delayed rectifier's conductance nor its activation were blocked by a number of pharmacological agents tested for this purpose. Therefore, experiments on Raia electroplaques were limited to membrane voltages more negative than -50 mV.

NEURALLY EVOKED POSTSYNAPTIC CURRENTS

Postsynaptic Current Waveform. Figure 18 shows voltage-clamp currents evoked by stimulating presynaptic nerves. These postsynaptic currents (PSC's) peak rapidly and then decay with a single exponential time constant. At a given membrane voltage, peak PSC increases with the strength and duration of the presynaptic stimulus. This increase occurs

Figure 18. Typical PSC's in a skate electroplaque at three different temperatures. Membrane voltage-clamped to -60 mV. An upward deflection indicates inward current. Stimulus artifacts occur five msec after the start of each trace.

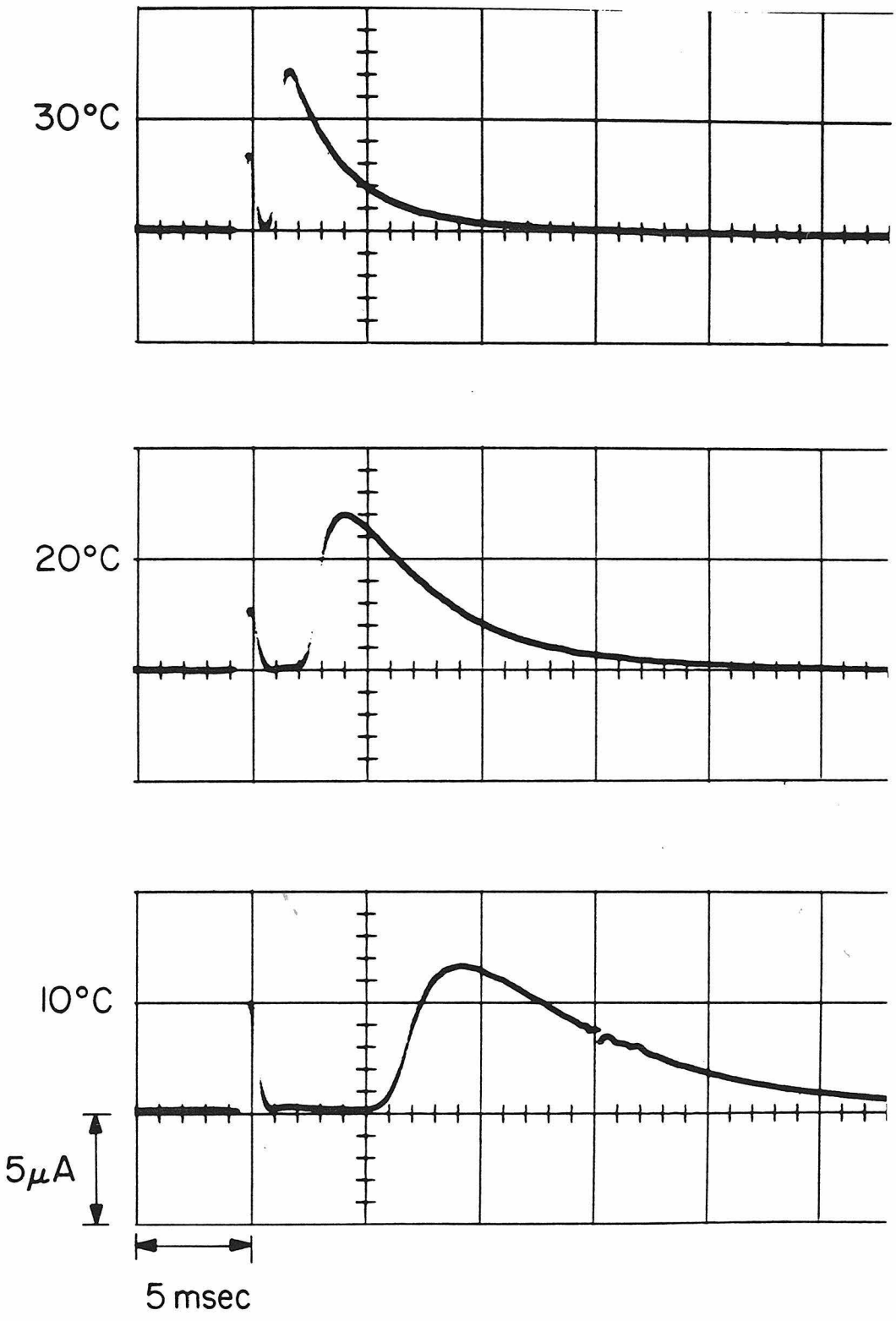
30°C
20°C
10°C
5μA
5 msec

in three to five distinct steps to a maximum peak PSC which varies from cell to cell. The stepwise response to presynaptic stimulation implies multiple innervation of each electroplaque. Multiple innervation is also indicated by anatomical studies (Bennett, 1961). When all other conditions are equal, once the presynaptic stimulus is set the PSC amplitude remains constant over the course of the experiment.

After the peak, PSC's decay along a simple exponential time course (Figure 19). The PSC decay rate, α, is the inverse time constant of this exponential decay and is measured as the slope of the semilogarithmic plot of PSC vs. time after the PSC peak.

Temperature Effects. Increasing the electroplaque's temperature decreases the time from presynaptic stimulus to PSC peak, the growth time (20% to 80%) of the PSC, and the PSC decay time constant (Figure 18). The first two processes have Q_{10}'s of approximately two. The temperature dependence of these processes is difficult to measure quantitatively because the PSC peak becomes broader and difficult to measure at low temperatures. However, the PSC decay can be measured with greater accuracy (Figure 19). At low temperatures, broadening of the PSC peak induces deviations from a simple exponential decay. This problem is avoided by analyzing only the later, exponential portions of the PSC decay. The Q_{10} of the PSC decay rate, α, is 1.95 at -100 mV (3 cells, each studied from 10° to 30°). In other words, the PSC decay rate doubles for each 10° rise in temperature.

Figure 19. Semilogarithmic plot of postsynaptic current vs. time after the PSC peak. Temperature, 21°. Membrane voltage, -72.5 mV. Slope of the indicated line is the decay rate of the PSC and equals 0.24 $msec^{-1}$.

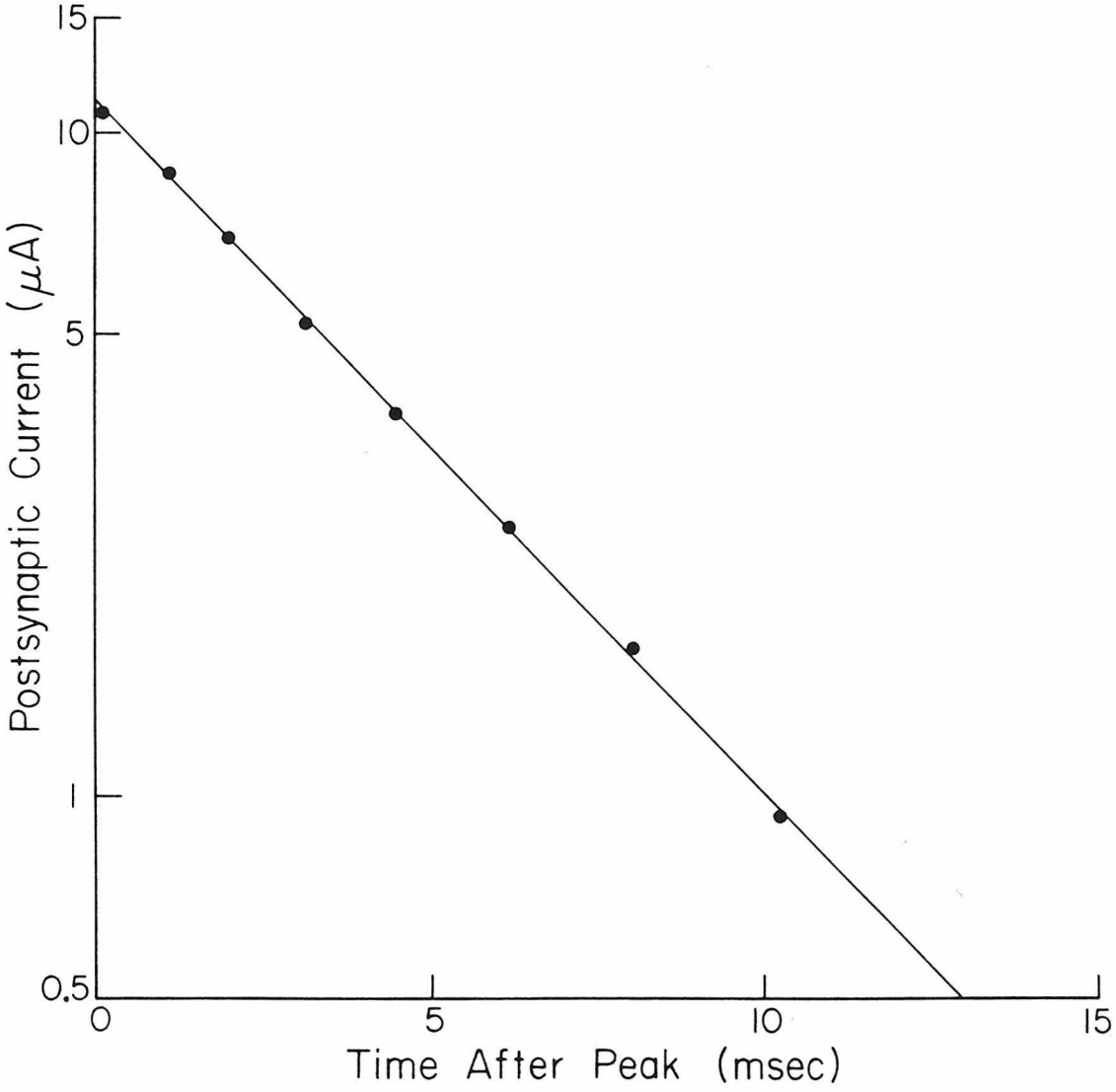
15
10
5
1
0.5
Postsynaptic Current (μA)
0
5
10
15
Time After Peak (msec)

PSC Decay Rates. PSC decay rate vs. membrane voltage is plotted in Figures 20a and 21a. The PSC decay rate does not change with voltages from -50 to -150 mV. Furthermore, the PSC decay rate is equally independent of membrane voltage at all temperatures from 10° to 30°.

Voltage dependence does not appear in smaller PSC's. The PSC decay rate does not change when the peak PSC is reversibly reduced during bath-application of d-tubocurarine (dTC). The PSC decay rate remains voltage independent when the peak PSC is reduced as much as four-fold (Figure 20). The PSC decay rate is also unchanged when the presynaptic stimulus is reduced in order to decrease the peak PSC. Again, the PSC decay rate remains voltage independent. Therefore, the PSC decay rate is independent of the PSC amplitude.

The PSC lengthens during bath application of the anticholinesterase agent neostigmine methylsulfate. During such drug applications, the PSC decay continues to follow a simple exponential time course, although the rate of PSC decay is reduced (Figure 21a). The PSC decay rate is not voltage dependent in any concentration of neostigmine below 10^{-3}M. There is little (<10%) change in peak PSC amplitude with neostigmine concentrations below 10^{-4}M (Figure 21b). Neostigmine concentrations greater than 5×10^{-4}M decrease the peak PSC. This decrease is not due to altered electrical excitability of the presynaptic terminals because the stimulus thresholds did not change. Similar effects of neostigmine have been observed in amphibian skeletal muscle (Magleby and Stevens, 1972a,b), and are generally attributed to competitive antagonism by neostigmine at the nicotinic receptor.

Figure 20. Effects of voltage and dTC on the PSC in *Raia* electroplaque. Open squares: control PSC's. Filled squares: PSC's during treatment with 10^{-5}M dTC. (a) Plot of PSC decay rate vs. membrane voltage. (b) Plot of peak PSC vs. membrane voltage. Arrow indicates the extrapolated value of the reversal potential at +18 mV. Passive currents have been subtracted. Temperature, 20°.

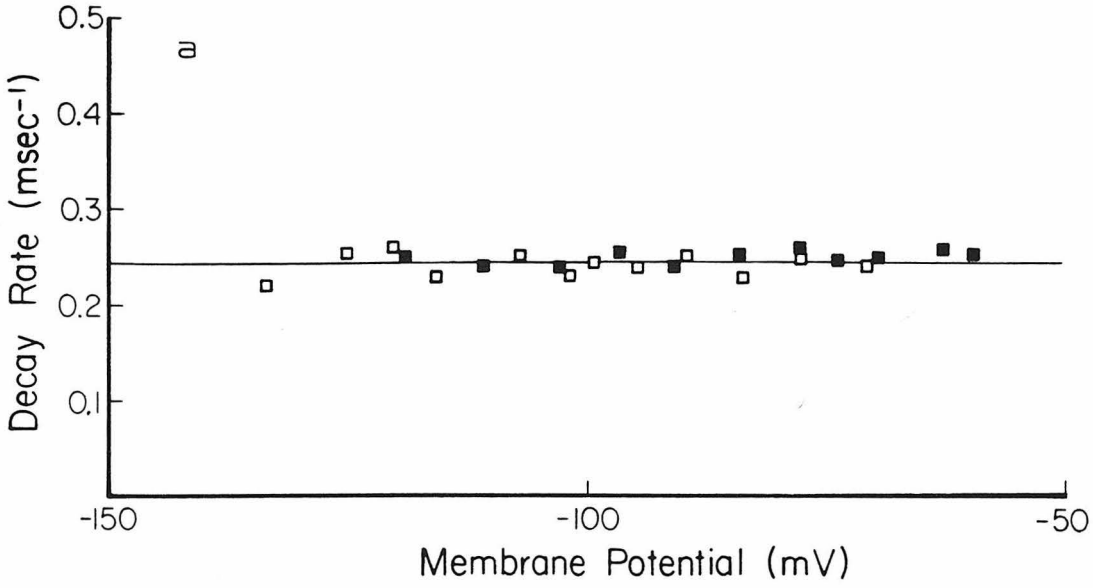
a
0.5
0.4
0.3
0.2
0.1
Decay Rate (msec⁻¹)
-150
-100
-50
Membrane Potential (mV)

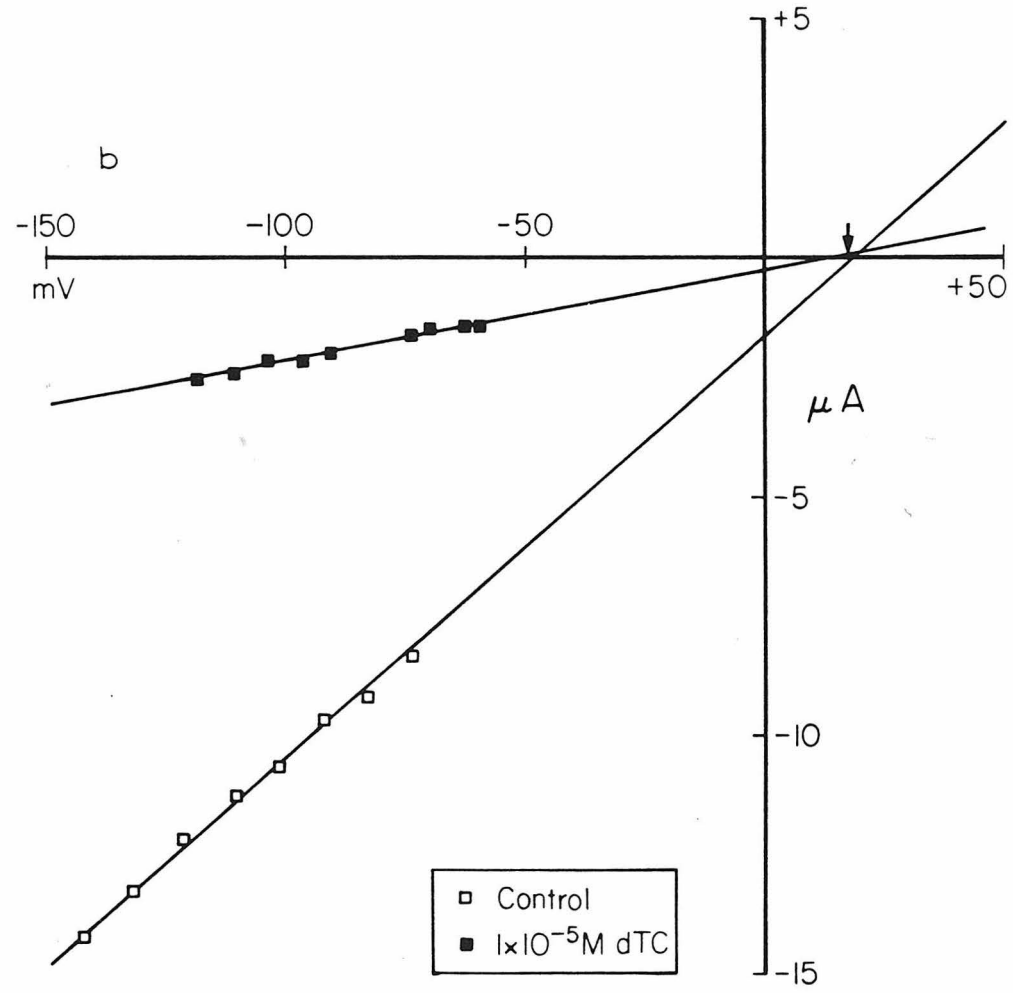
b
-150
-100
-50
mV
+50
+5
μA
-5
-10
-15
Control
1×10⁻⁵M dTC

Peak PSC vs. Voltage Relations. Peak PSC increases linearly as the membrane voltage becomes more negative (Figures 20b and 21b). Such linear current vs. voltage relations imply that peak postsynaptic conductance is independent of membrane voltage. Assuming that the peak PSC vs. voltage relation continues to be linear at voltages more positive than -50 mV, the reversal potential of the PSC can be estimated by extrapolating the peak PSC vs. voltage relation to zero current. This extrapolated reversal potential is +5 ± 10 mV (mean ± SD, 7 cells) at 20°. Neither the linearity of the peak PSC vs. voltage relation nor the extrapolated PSC reversal potential are changed during application of dTC (Figure 20b), although dTC does decrease the slope of the peak PSC vs. voltage relation, indicating a decreased peak conductance. Similarly, neither the linearity, extrapolated reversal potential, nor slope of the peak PSC vs. voltage relation are changed by concentrations of neostigmine sufficient to reduce the PSC decay rate (Figure 21b).

BATH-APPLIED AGONIST

Measurement of Agonist-Induced Current. Raia electroplaques depolarize when a cholinergic agonist, such as carbachol, is applied in the extracellular bath. Depolarization to -50 mV activates delayed rectification, and the electroplaque's conductance dramatically increases. Delayed rectification might have been prevented during agonist application by using the voltage-clamp circuit to provide continuous hyperpolarization. Unfortunately, the large currents required could not be maintained over the several minutes necessary for

Figure 21. Effects of voltage and acetylcholinesterase inhibitors on the PSC. Open circles: control PSC's. Filled circles: PSC's during treatment with 3×10^{-5}M neostigmine methylsulfate. (a) Plot of PSC decay rate vs. membrane voltage. (b) Plot of peak PSC vs. membrane voltage. Arrow indicates the extrapolated reversal potential at +40 mV. Passive currents have been subtracted. Temperature, 13°.

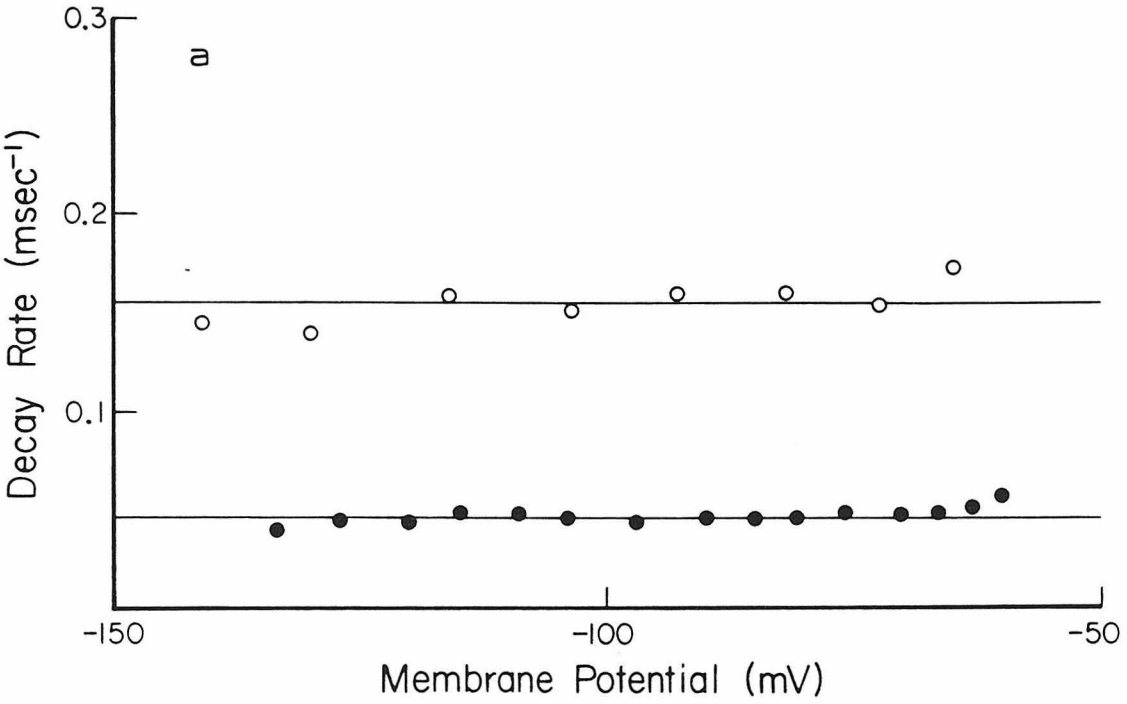
a
0.3
0.2
0.1
Decay Rate (msec⁻¹)
-150
-100
-50
Membrane Potential (mV)

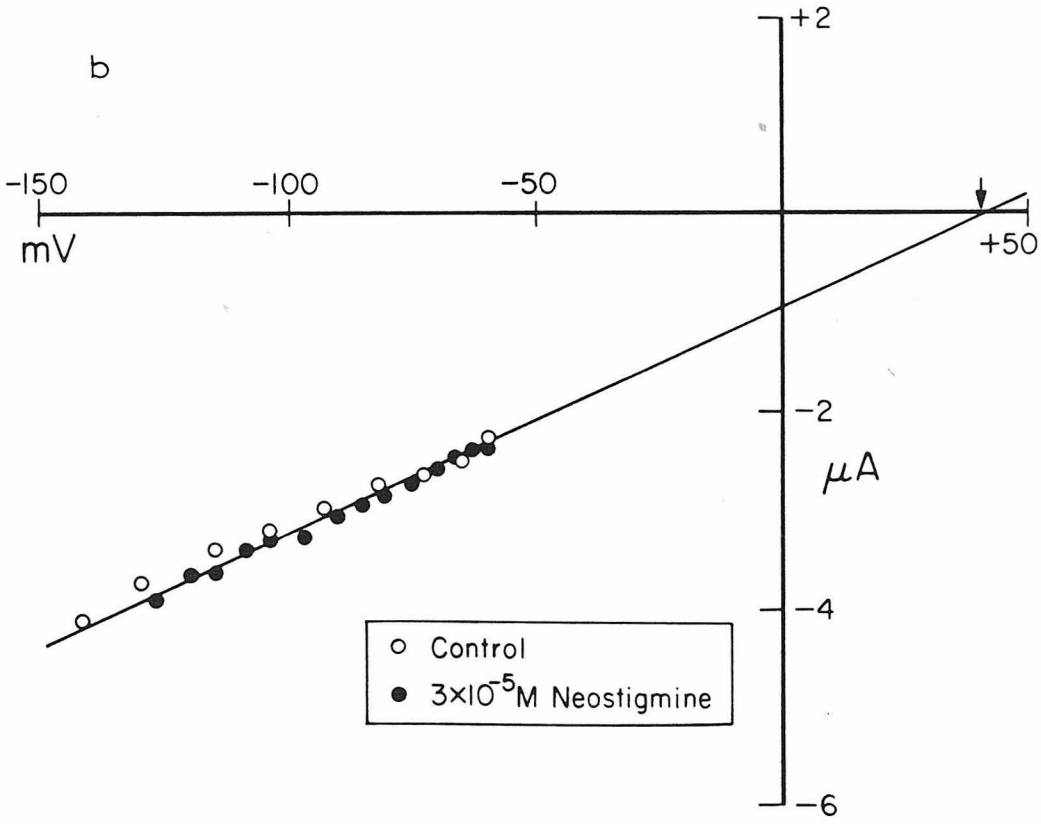
b
+2
-150
-100
-50
mV
+50
-2
μA
-4
-6
Control
3×10⁻⁵M Neostigmine

agonist equilibration at the electroplaque. Steady-state depolarization increases with agonist concentration. Therefore, delayed rectification could be avoided by applying only low agonist concentrations to Raia electroplaques. Low agonist concentrations were applied to the electroplaque either (a) by adding a low concentration of agonist to the bath and waiting for equilibrium response or (b) by measuring agonist-induced conductance before equilibration of a higher agonist concentration. Drug equilibration requires several minutes in Raia electroplaques due to connective tissue diffusion barriers. This long equilibration time permits brief measurements of agonist-induced conductance at intervals during equilibration of the agonist. During each measurement the agonist concentration is essentially constant, but unknown.

In 3 μM carbachol, the electroplaque undergoes a barely detectable depolarization. In 6 μM carbachol, steady-state depolarization is approximately 15 mV. In 9 μM carbachol, depolarization eventually reaches threshold for activation of delayed rectification. The 9 μM experiments were monitored at various times during agonist equilibration (Figure 22). Carbachol is not readily hydrolysed by acetylcholinesterase, so agonist concentration does not change after equilibration. Further, agonist-induced conductance did not desensitize, probably because of the low agonist concentrations used in the equilibration experiments (Adams, 1975a; Lester et al., 1975).

Voltage Dependence of Agonist-Induced Current. Without agonist, the

Figure 22. Voltage-clamp current vs. membrane voltage. Control currents indicate the passive membrane's conductance. Currents during carbachol application are shown at 2, 9, and 13 min after introduction of 9 μM carbachol. Right-hand arrow indicates the extrapolated reversal potential for agonist-induced current (-5 mV). Left-hand arrow indicates the altered reversal potential when delayed rectification is active (curve at 13 min). Temperature, 20°.

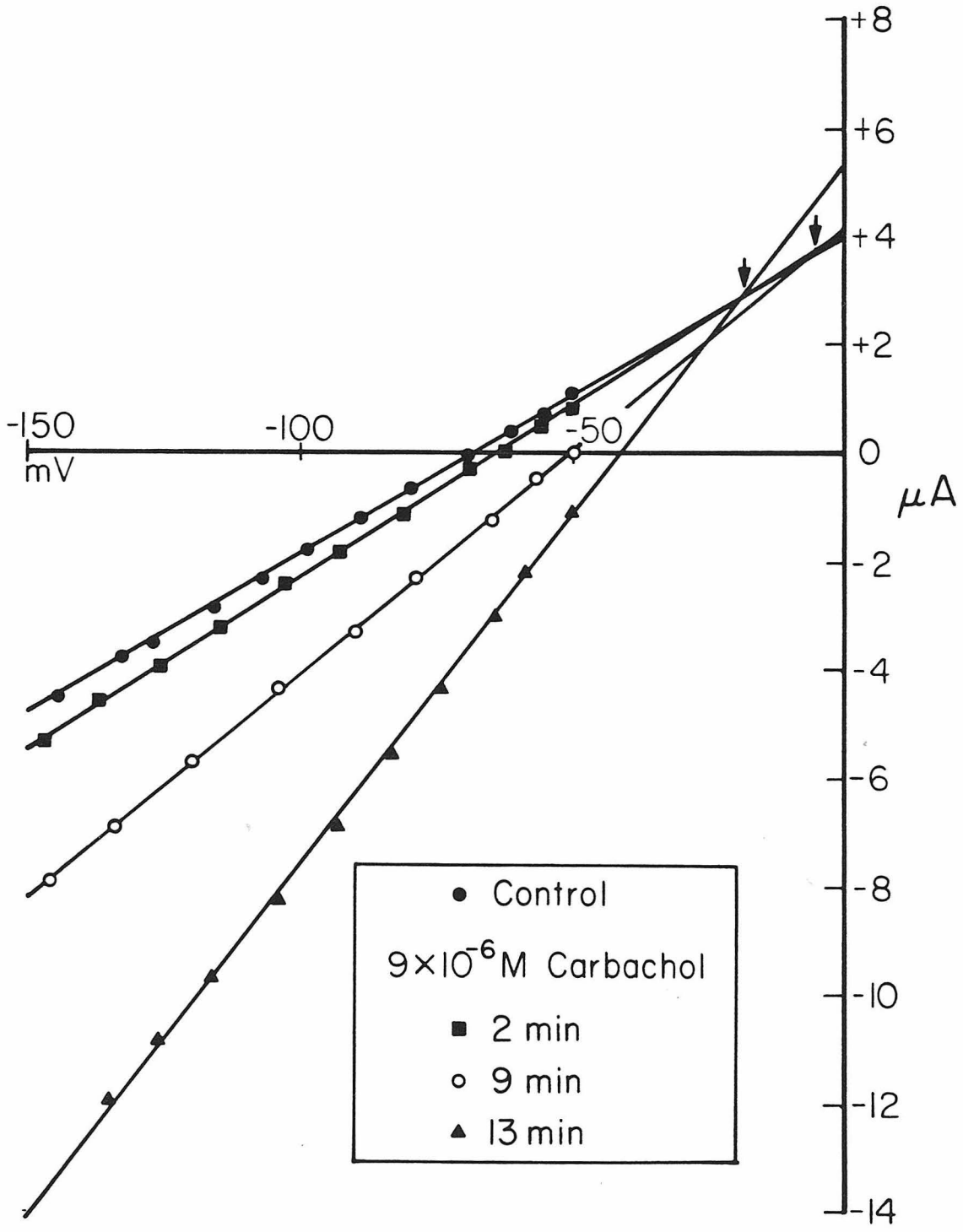
+8
+6
+4
+2
0
-2
-4
-6
-8
-10
-12
-14
μA
-150
mV
-100
-50
• Control
9×10⁻⁶M Carbachol
■ 2 min
○ 9 min
▲ 13 min

electroplaque's current vs. voltage relation is linear from -50 to -150 mV. Carbachol increases the electroplaque's conductance, but the current vs. voltage relation remains linear (Figure 22). Therefore, the steady-state, agonist-induced conductance is independent of membrane voltage, at least over the range of -50 to -150 mV. Provided that the current vs. voltage relation remains linear at voltages more positive than -50 mV, the reversal potential for agonist-induced current can be estimated by extrapolating the current vs. voltage relations with and without agonist to a point of intersection. This extrapolated reversal potential is -10 ± 10 mV (mean ± SD, 8 cells) at 20°. In the electroplaque of Figure 22, this reversal potential was constant during agonist equilibration, until the resting potential depolarized beyond -50 mV (13 min after agonist application). The electroplaque's conductance then sharply increased as delayed rectification was activated, and the extrapolated intercept with control currents became more negative. This new intercept presumably represents a combined value of reversal potentials for agonist-induced current (-10 mV) and for delayed rectifier current (probably $\leq$ -50 mV).

DISCUSSION

Nicotinic responses in Raia erinacea electroplaques are similar in many ways to nicotinic responses in skeletal muscle fibers and in Electrophorus electroplaques. For example, cholinergic agonists reversibly increase Na^+ and K^+ conductance in Raia electroplaques (Brock and Eccles, 1958). The nicotinic antagonists dTC and Naja nigricollis α-toxin block the PSC in Raia electroplaques (Schoffeniels,

1958; Lester, 1970, 1972). The Raia electroplaque responds to the cholinergic agonist carbachol in concentrations similar to those effective on skeletal muscle and on Electrophorus electroplaques (Adams, 1975a,b; Lester et al., 1975). Finally, acetylcholinesterase is present in Raia electroplaques, and esterase activity shortens the PSC time course.

Despite these similarities to amphibian skeletal muscle and to Electrophorus electroplaques, nicotinic responses in Raia erinacea electroplaques have several unique properties. First, the PSC decay rate is independent of membrane voltage. Second, agonist-induced conductance is independent of membrane voltage. And third, PSC decay rates are less temperature dependent than the PSC decay rates in amphibian skeletal muscle or in Electrophorus electroplaques.

Of primary interest is the relation between these observed responses and the rate-limiting steps at the nicotinic receptor. Certain assumptions about the nicotinic receptor greatly simplify the description of observed kinetics and equilibria in terms of reaction rates. (a) Nicotinic receptors can assume only one "open" state which contributes an ohmic conductance of γ to the total agonist-induced conductance. (b) All other receptor states are "closed" and do not contribute any conductance. These two assumptions imply that agonist-induced conductance is directly porportional to the fraction of the receptor population in the open state. Further, at any given voltage, the agonist-induced current, I, is directly porportional to the agonist-induced conductance and hence to the number of open receptors.

(c) The Raia electroplaque contains only one receptor population, r, which is equally accessible to either neurally released agonist or bath-applied agonist. This assumption allows direct comparison of results obtained from PSC's and from bath application of agonist.
(d) Relaxations of the receptor population are governed by unidirectional rate constants: a net opening rate, β , and a net closing rate, α. This is a simplified form of the equations derived in PART ONE for Electrophorus electroplaques (Sheridan and Lester, 1975).

Voltage Independence of PSC Decay Rates. In Raia electroplaques the PSC decays along a simple exponential time course, as do PSC decays in amphibian skeletal muscle fibers and in Electrophorus electroplaques. However, in the latter two preparations the PSC decay rate decreases as the membrane is hyperpolarized. This voltage dependence varies with temperature but generally amounts to about a factor of three for every 100 mV of hyperpolarization (Magleby and Stevens, 1972a,b; Kordas, 1972b; Gage and McBurney, 1975; Sheridan and Lester, 1975, 1977). If PSC decays in Raia electroplaques were as voltage dependent, the PSC decay rate would have changed three-fold over the 100 mV range studied. Such a change would have been obvious in the experiments of Figures 20a and 21a. There was, in fact, no systematic change in PSC decay rate with membrane voltage to an accuracy of ± 10%. Like the Raia electroplaque, a number of preparations have voltage independent PSC decay rates. These preparations include the squid giant synapse (Llinas et al., 1974), a glutamate synapse in locust muscle (Anwyl and Usherwood, 1976), a cholinergic synapse in Aplysia buccal ganglion

(Gardner, 1975, 1976), and tonic skeletal muscle fibers in the ribbon snake (Dionne and Parsons, 1977).

The interpretation of the PSC decay rate in terms of reaction rates depends on the acetylcholine concentration in the cleft during PSC decay. Like the PSC in amphibian skeletal muscle and Electrophorus electroplaque, the PSC in Raia electroplaque is lengthened by acetylcholinesterase inhibition because neurally released acetylcholine is no longer rapidly hydrolysed and must leave the synaptic cleft by diffusion alone. The rate of acetylcholine loss is further slowed by multiple binding of acetylcholine to nicotinic receptors. Application of dTC effectively reduces the receptor "concentration", thus reducing the extent of multiple binding with acetylcholine, increasing the rate of acetylcholine loss from the cleft, and increasing the PSC decay rate. The limit to which multiple binding can be reduced with dTC is a single event; the corresponding limit of the PSC decay rate is the closing rate for the receptors. In amphibian skeletal muscle fibers and in Electrophorus electroplaques treated with acetylcholinesterase inhibitors, dTC application increases the PSC decay rate to a value nearly equal to that obtained before acetylcholinesterase inhibition (Katz and Miledi, 1973; Sheridan and Lester, 1977). When acetylcholinesterase is functional in Raia electroplaques, the PSC decay rate is unchanged during dTC application (Figure 20a), implying that no multiple binding occurs and that there is little or no acetylcholine in the synaptic cleft during PSC decay. Therefore, in Raia electroplaques with functional acetylcholinesterase, the PSC decay rate, α, is the closing rate for receptors. Since the PSC decay rate is voltage

independent, the closing rate of these nicotinic receptors must be voltage insensitive.

Voltage Independence of Agonist-Induced Conductance. Agonist-induced conductance can be measured during bath application of agonist or during the peak PSC. Aside from any differences in the agonist used, these two measures of agonist-induced conductance are not equivalent because the time course of agonist application differs markedly. During bath application the agonist concentration changes slowly and the receptor population is always at equilibrium. During the PSC, the agonist concentration changes rapidly with respect to the receptor rates. Consequently, the results from bath-applied agonist and peak PSC must be examined separately.

In Raia electroplaques, bath-applied carbachol induces a steady-state current that increases linearly as the electroplaque is hyperpolarized. This agonist-induced current can be described by the equation:

$$I = r\gamma(V - E)\left[\frac{\delta}{\delta + \alpha}\right]^2 \qquad (26)$$

where r is the receptor population, γ is the unit receptor conductance, V is the membrane voltage, E is the reversal potential, δ is the opening rate for receptors, and α is the closing rate for receptors. The opening rate, δ, increases with increasing agonist concentration (Adams, 1975b; Sheridan and Lester, 1975, 1977). In amphibian skeletal muscle fibers and in Electrophorus electroplaques, steady-state, agonist-induced current increases more than linearly as the membrane

is hyperpolarized (Adams, 1975b; Dionne and Stevens, 1975; Lester et al., 1975; Sheridan and Lester, 1975, 1977; Lassignal and Martin, 1976, 1977). The reason for this voltage dependent conductance is that the closing rate, α, decreases with hyperpolarization, while the opening rate, δ, changes only slightly with voltage. Consistent with this interpretation and with equation (26), agonist-induced conductance becomes less voltage dependent at high agonist concentrations because δ becomes larger. In Raia electroplaques, however, steady-state, agonist-induced current varies linearly with voltage even though only low agonist concentrations were used (Figure 22). Therefore, in Raia electroplaques, the opening rate, δ, and the closing rate, α, for nicotinic receptors must be equally voltage sensitive. Since PSC decay rates indicate that the closing rate is voltage insensitive, the opening rate must also be voltage insensitive.

Like the steady-state current during bath application of agonist, the peak PSC varies linearly with the membrane voltage. However, unlike the case during bath application, the acetylcholine concentration in the synaptic cleft is unknown during the growth phase of the PSC. Two alternative hypotheses must be considered. (a) In amphibian skeletal muscle fibers and in Electrophorus electroplaques, several investigators have calculated that agonist concentration is high enough near a site of presynaptic release to open most of the adjacent receptors (Kuffler and Yoshikami, 1975a,b; Fertuck and Salpeter, 1976; Lester et al., 1976). If this is also true in Raia electroplaques, then equation (26) predicts that peak PSC should equal $r\gamma(V - E)$. In this case, the linear peak PSC vs. voltage relation in Raia electroplaques indicates only that the

conductance contributed by a single receptor, γ, is ohmic at voltages more negative than -50 mV. (b) If, on the other hand, only a few receptors near a presynaptic release site open during the growth phase of the PSC, then the time course of acetylcholine release must be considered. The duration of the PSC growth phase is much less than the time constant for PSC decay. Since the time constant of PSC decay equals the mean lifetime of the open state of the receptor (Magleby and Stevens, 1972a,b; Anderson and Stevens, 1973), very few of the receptors opened during the growth phase of the PSC have a chance to close before the PSC peak. Consequently, the peak PSC represents the integrated value of the opening rate, β, during the entire growth phase of the PSC (Dionne and Stevens, 1975; Lester et al., 1976). In amphibian skeletal muscle fibers the peak PSC increases less than linearly as the membrane is hyperpolarized. This nonlinearity is attributed to a voltage sensitive opening rate for nicotinic receptors (Dionne and Stevens, 1975). In Electrophorus electroplaques the peak PSC increases linearly as the membrane is hyperpolarized beyond -30 mV. The opening rate is thought to be voltage insensitive in Electrophorus electroplaque receptors (Sheridan and Lester, 1977). The peak PSC vs. voltage relation is also linear in Raia electroplaques (Figures 20b and 21b). Thus, hypothesis (b) implies that the opening rate is voltage insensitive in Raia electroplaque receptors.

The accuracy of the measured reversal potential depends on the voltage sensitivity of agonist-induced conductance. Equation (26) predicts that agonist-induced current equals zero when V equals E. In Raia electroplaques, agonist-induced current could not be measured at

voltages more positive than -50 mV, where this reversal potential apparently lies. Therefore, the reversal potential could only be measured by extrapolation from the current vs. voltage relations at voltages more negative than -50 mV. Equation (26) also predicts that such extrapolation yields an accurate reversal potential only if γ, δ, and α are voltage insensitive in the measured range of voltages. Hypothesis (a) for the peak PSC implies that γ is voltage independent at voltages more negative than -50 mV. Further, the kinetics of the receptor, δ and α, are voltage insensitive from -150 to -50 mV. Therefore, extrapolation probably indicates a correct reversal potential in Raia electroplaques.

The extrapolated reversal for peak PSC was +5 ± 10 mV (mean ± SD) at 20°, and the extrapolated reversal potential in bath-applied carbachol was -10 ± 10 mV (mean ± SD) at 20°. The difference between these two estimates of the reversal potential is not significant. Occasionally the extrapolated peak PSC reversal potential was much more positive than the average (see Figure 21b). Such cells also had postsynaptic potentials which overshot 0 mV. These large postsynaptic potentials are consistent with a positive reversal potential and have been reported in Raia electroplaques by other investigators (Brock and Eccles, 1958).

Temperature and the PSC Decay Rate. In Raia electroplaques, the PSC decay rate has an unusually low Q_{10} of 1.95. In amphibian skeletal muscle and in Electrophorus electroplaque, the PSC decay rate has a Q_{10} of about 3; the exact value varies with membrane voltage (Magleby and Stevens, 1972b; Sheridan and Lester, 1975). Although it is low for a

nicotinic synapse, the Raia electroplaque's Q_{10} is still too large to be consistent with a diffusion-limited process (Dreyer and Peper, 1975b) and nearly equals the Q_{10} of the PSC decay at certain glutamate synapses (Anderson et al., 1976; Anwyl and Usherwood, 1976).

It is possible to relate the low Q_{10} and the voltage independence of the PSC decay rate in Raia electroplaques. In general, a low Q_{10} implies a low activation energy for the associated chemical reaction step. Making the reasonable assumption that the open to closed transition of nicotinic receptors involves a free energy change:

$$\Delta G = T\Delta S + \Delta E \tag{27}$$

where T is the absolute temperature, then according to the activated complex theory the transition rate is:

$$\alpha = \frac{kT}{h} \exp(\Delta S/R) \exp(-\Delta E/RT) \tag{28}$$

where k, h, and R are constants (Gardner, 1969). Voltage is expected to affect a nicotinic receptor primarily by changing the activation energy, ΔE. For instance, if the rate-limiting step in receptor closing involves a dipole moment change, μ, as suggested by Magleby and Stevens (1972b) for amphibian skeletal muscle, then ΔE has the form:

$$\Delta E = \Delta E_o + N(V - V_o)\mu/M \tag{29}$$

where N and M are constants, where ΔE_o is positive and voltage insensitive, and where V_o is a correction for membrane surface charge (Magleby and Stevens, 1972b; Gage et al., 1975). If μ equals zero in Raia electroplaque receptors, this theory explains how α is both voltage insensitive and less temperature dependent than in amphibian skeletal muscle fibers, where $\mu < 0$ and the PSC decay rate is voltage sensitive. In amphibian skeletal muscle, α has a lower Q_{10} as $V - V_o$

approaches zero. Experimentally, PSC decay rates in amphibian skeletal muscle fibers at 0 mV and Raia electroplaques at all voltages have equal Q_{10}'s for the PSC decay rate (Magleby and Stevens, 1972b). If the only difference between these two preparations is μ, then ΔE_o is the same for nicotinic receptors in Raia electroplaques and amphibian skeletal muscle. Furthermore, this implies that V_o equals zero in amphibian skeletal muscle. Unfortunately, this simple analysis fails to account for the five-fold difference between the magnitude of the PSC decay rate in Raia electroplaque at all voltages and in amphibian skeletal muscle at 0 mV.

Space Clamp in Raia Electroplaques. Space clamp is a condition of spatially uniform membrane voltage. Failure of space clamp leads to some serious artifacts in voltage-clamp records of conductance changes. For instance, when an amphibian skeletal muscle fiber is voltage-clamped one length constant away from the endplate, PSC decay rates appear to be voltage insensitive (Magleby and Stevens, 1972a). Therefore, space-clamp failure could account for the observed lack of voltage sensitivity in Raia electroplaque receptors.

There are several reasons to believe that Raia electroplaques were adequately space clamped. First, equations (24) and (25) predict that the passive membrane in Raia electroplaques is space clamped. Second, PSC decay rates are independent of PSC amplitude (Figure 20). Since space-clamp failure is more likely during conditions of high membrane

conductance, one would expect evidence of voltage independence only with larger PSC's. Third, agonist-induced current increased as the electroplaque was hyperpolarized, which indicates that the membrane voltage near the receptors changed in response to the applied current. And fourth, the extrapolated reversal potentials for agonist-induced current are consistent with observed postsynaptic potentials in Raia electroplaques (Brock and Eccles, 1958) as well as with reversal potentials in amphibian skeletal muscle (Magleby and Stevens, 1972a) and Electrophorus electroplaque (Lester et al., 1975). Space-clamp failure would have made the extrapolated reversal potential appear to be more positive than the actual reversal potential at the receptors. Thus, to all indications, Raia electroplaques were adequately space clamped during agonist-induced conductance changes. Consequently, the observed voltage insensitivity of receptor opening and closing rates is probably an inherent property of the nicotinic receptor in Raia electroplaques.

Teleology of Voltage Sensitivity. Voltage control of nicotinic receptor rates seems advantageous under certain conditions (Lester et al., 1976). For example, a voltage-sensitive nicotinic receptor could prevent shunting of an electrically excitable, inward current in the same cell. Also, depolarization by such an inward current could shift the nicotinic receptor population toward the closed state and shorten the postsynaptic event. These advantages do not apply to Raia electroplaques. Raia electroplaques have no electrically excitable inward current, and all depolarization is due to the PSC. Thus, it would be counterproductive to decrease nicotinic receptor conductance as the electroplaque

depolarizes in response to that same conductance. Far from being an isolated case, the voltage-independent PSC's in Raia electroplaque appear to be typical of cells which lack an electrically excitable inward current. For example, both invertebrate muscle fibers and tonic skeletal muscle fibers are electrically inexcitable. Both preparations also have voltage-independent PSC's (Anwyl and Usherwood, 1976; Dionne and Parsons, 1977).

REFERENCES

Adams, P.R. 1975a. A study of desensitization using voltage-clamp. Pflugers Arch. 360: 135-144.

Adams, P.R. 1975b. An analysis of the dose-response curve at voltage-clamped frog endplates. Pflugers Arch. 360: 145-153.

Adams, P.R. 1975c. Kinetics of agonist conductance changes during hyperpolarization at frog endplates. Br. J. Pharmac. 53: 308-310.

Adams, P.R. 1976. Voltage dependence of agonist responses at voltage-clamped frog endplates. Pflugers Arch. 361: 145-151.

Adams, P.R. 1977. Relaxation experiments using bath-applied suberyldicholine. J. Physiol. 268: 271-289.

Anderson, C.R. and C.F. Stevens. 1973. Voltage clamp analysis of acetylcholine induced end-plate current fluctuations at frog neuromuscular junction. J. Physiol. 235: 655-691.

Anderson, C.R., S.G. Cull-Candy and R. Miledi. 1976. Glutamate and quisqualate noise in voltage-clamped locust muscle fibres. Nature 261: 151-153.

Anwyl, R. and P.N.R. Usherwood. 1976. Factors affecting the time course of decay of excitatory postsynaptic currents at a glutamate synapse. J. Physiol. 254: 46-47P.

Armstrong, C.M. 1975. Ionic pores, gates, and gating currents. Quart. Rev. Biophys. 7: 179-210.

Bamberg E. and P. Lauger. 1973. Channel formation kinetics of gramicidin A in lipid bilayer membranes. J. Membrane Biology 11: 177-194.

Bennett, M.V.L. 1961. Modes of operation of electric organs. Annal. N.Y. Acad. Sci. 94: 458-509.

Bonner, R., F.J. Barrantes, and T.M. Jovin. 1976. Kinetics of agonist-induced intrinsic fluorescent changes in membrane-bound acetylcholine receptor. Nature 263: 429-431.

Brock, L.G. and R.M. Eccles. 1958. The membrane potentials during rest and activity of the ray electroplate. J. Physiol. 142: 251-274.

Cartaud, J., E.L. Benedetti, J.B. Cohen, J.B. Meunier, and J.P. Changeux. 1973. Presence of a lattice structure in membrane fragments rich in nicotinic receptor protein from the electric organ of Torpedo marmorata. F.E.B.S. Letters 33: 109-113.

Changeux, J.P., L. Benedetti, J.P. Bourgeois, A. Brisson, J. Cartaud, P. Devaux, H. Grunhagen, M. Moreau, J.P. Popot, A. Sobel, and M. Weber. 1975. Some structural properties of the cholinergic receptor protein. C.S.H. Symposia 40: 211-230.

Changeux, J.P., M. Kasai, and C.Y. Lee. 1970. Use of a snake venom toxin to characterize the cholinergic receptor protein. Proc. Natl. Acad. Sci. USA 67: 1241-1247.

Changeux, J.P. and T.R. Podleski. 1968. On the excitability and cooperativity of the electroplax membrane. Proc. Natl. Acad. Sci. USA 59: 944-950.

Cole, K.S. 1968. Membranes, ions, and impulses. U. of Calif. Press, Berkeley, California.

Colquhoun, D., V.E. Dionne, J.H. Steinbach, and C.F. Stevens. 1975. Conductance of channels opened by acetylcholine-like drugs in muscle end-plate. Nature 253: 204-206.

Colquhoun, D., W.A. Large, and H.P. Rang. 1977. An analysis of the action of a false transmitter at the neuromuscular junction. J. Physiol. 263: 388-400.

Dionne, V.E. and R.L. Parsons. 1977. End plate currents differ at twitch and slow fiber neuromuscular junctions. J. Gen. Physiol. (abstract in press).

Dionne, V.E. and R.L. Ruff. 1977. Endplate current fluctuations reveal only one channel type at frog neuromuscular junction. Nature 266: 263-265.

Dionne, V.E. and C.F. Stevens. 1975. Voltage dependence of agonist effectiveness at the frog neuromuscular junction. J. Physiol. 251: 245-270.

Dreyer, F. and K. Peper. 1975a. Density and dose-response curve of acetylcholine receptors in frog neuromuscular junction. Nature 253: 641-643.

Dreyer, F. and K. Peper. 1975b. Analysis of cooperitivity of drug-receptor interaction by quantitative iontophoresis at frog motor end plates. C.S.H. Symposia 40: 187-192.

Eigen, M. and L. deMaeyer. 1974. Theoretical basis of relaxation spectrometry. In G.G. Hammes (ed.) Investigation of rates and mechanisms of reactions, Part II. Wiley, New York. 63-146.

Fertuck, H.C. and M.M. Salpeter. 1976. Quantitation of junction and extrajunctional acetylcholine receptors by electron microscope autoradiography. J. Cell. Biol. 69: 144-158.

Fromm, H.J. 1975. Initial rate enzyme kinetics. Springer-Verlag, New York. 236-244.

Gage, P. 1976. Generation of endplate potentials. Physiol. Rev. 56: 177-247.

Gage, P.W. and R.N. McBurney. 1975. Effects of membrane potential, temperature and neostigmine on the conductance change caused by a quantum of acetylcholine at the toad neuromuscular junction. J. Physiol. 244: 385-407.

Gage, P.W., R.N. McBurney, and G.T. Schneider. 1975. Effects of some aliphatic alcohols on the conductance change caused by a quantum of acetylcholine at the toad end plate. J. Physiol. 244: 909-929.

Gardner, D. 1975. A self-inhibitory synaptic potential in Aplysia buccal ganglia. Neurosci. Abst. 1: 571.

Gardner, D. 1976. Decrement and desensitization of a self-inhibitory synaptic potential in Aplysia buccal ganglia. Neurosci. Abst. 2: 1004.

Gardner, W.C. 1969. Rates and mechanisms of chemical reactions. W. A. Benjamin, Menlo Park, California. 150-173.

Grunhagen, H.H., M. Iwatsabu, and J.P. Changeux. 1976. Changements rapides de fluorescence observes en presence d'agoniste cholinergique avec des fragments de membranes riches en recepteur cholinergique de Torpedo marmorata marque avec la quinacrine. C.R. Acad. Sci. 283: 1105-1108.

Harris, A.L., J.O. Schairer, and M.V.L. Bennett. 1976. Calcium activated rectification in skate electroplaques. Neurosci. Abst. 2: 179.

Hammes, G.G. and C.W. Wu. 1974. Kinetics of allosteric enzymes. Ann. Rev. Biophys. Bioeng. 3: 1-33.

Hille, B., M.V.L. Bennett, and H. Grundfest. 1965. Voltage clamp measurements of the Cl-conductance changes in skate electroplaques. Biol. Bull. 129: 407-408.

Hodgkin, A.L. and A.F. Huxley. 1952. The dual effect of membrane potential on sodium conductance in the giant axon of Loligo. J. Physiol. 116: 497-506.

Jack, J.J.B., D. Noble, and R.W. Tsien. 1975. Electric current flow in excitable cells. Clarendon, Oxford. 83-91.

Karlin, A. 1967a. On the application of "a plausible model" of allosteric proteins to the receptor for acetylcholine. J. Theoret. Biol. 16: 306-320.

Karlin, A. 1967b. Permeability and internal concentration of ions during depolarization of the electroplax. Proc. Natl. Acad. Sci. USA 58: 1162-1167.

Karlin, A. and D. Cowburn. 1973. The affinity-labeling of partially purified acetylcholine receptor from electric tissue of Electrophorus. Proc. Natl. Acad. Sci. USA 70: 3636-3640.

Karlin, A., C.L. Weill, M.G. McNamee, and R. Valderrama. 1975. Facets of the structures of acetylcholine receptors from Electrophorus and Torpedo. C.S.H. Symposia 40: 203-210.

Katz, B. and R. Miledi. 1972. The statistical nature of the acetylcholine potential and its molecular components. J. Physiol. 224: 665-699.

Katz, B. and R. Miledi. 1973. The binding of acetylcholine to receptors and its removal from the synaptic cleft. J. Physiol. 231: 549-574.

Katz, B. and S. Thesleff. 1957. A study of the "desensitization" produced by acetylcholine at the motor end-plate. J. Physiol. 138: 63-80.

Kirschner, K. 1971. Kinetic analysis of allosteric enzymes. Curr. Topics Cellular Regulation 3: 167-210.

Kirschner, K., M. Eigen, R. Bittman, and B. Voigt. 1966. The binding of nicotinamide-adenine dinucleotide to yeast D-glyceraldehyde-3-

phosphate dehydrogenase. Proc. Natl. Acad. Sci. USA 56: 1661-1667.

Kirschner, K., E. Gallego, I. Schuster, and D. Goodall. 1970. Cooperative binding of nicotinamide-adenine dinucleotide to yeast glyceraldehyde-3-phosphate dehydrogenase. J. Molec. Biol. 58: 29-50.

Kordas, M. 1968. A study of the end-plate potential in sodium deficient solution. J. Physiol. 198: 81-90.

Kordas, M. 1972a. An attempt at an analysis of the factors determining the time course of the end-plate current. I. The effects of prostigmine and of the ratio of Mg^{++} to Ca^{++}. J. Physiol. 224: 317-332.

Kordas, M. 1972b. An attempt at an analysis of the factors determining the time course of the end-plate current. II. Temperature. J. Physiol. 224: 333-348.

Koshland, D.E. and K.E. Neet. 1968. The catalytic and regulatory properties of enzymes. Ann. Rev. Biochem. 37: 359-410.

Koshland, D.E., G. Nemethy, and D. Filmer. 1966. Comparison of experimental binding data and theoretical models in proteins containing subunits. Biochem. 8: 365-385.

Kuffler, S.W. and D. Yoshikami. 1975a. The distribution of acetylcholine sensitivity at the post-synaptic membrane of vertebrate skeletal twitch muscles. J. Physiol. 244: 703-730.

Kuffler, S.W. and D. Yoshikami. 1975b. The number of transmitter molecules in a quantum. J. Physiol. 251: 265-282.

Lassignal, N. and A.R. Martin. 1976. Reversal of acetylcholine potentials in eel electroplaque. Science 191: 464-466.

Lassignal, N. and A.R. Martin. 1977. Effect of acetylcholine on post-junctional membrane permeability in eel electroplaque. J. Gen. Physiol. 70: 23-36.

phosphate dehydrogenase. Proc. Natl. Acad. Sci. USA 56: 1661-1667.

Kirschner, K., E. Gallego, I. Schuster, and D. Goodall. 1970. Cooperative binding of nicotinamide-adenine dinucleotide to yeast glyceraldehyde-3-phosphate dehydrogenase. J. Molec. Biol. 58: 29-50.

Kordas, M. 1968. A study of the end-plate potential in sodium deficient solution. J. Physiol. 198: 81-90.

Kordas, M. 1972a. An attempt at an analysis of the factors determining the time course of the end-plate current. I. The effects of prostigmine and of the ratio of Mg^{++} to Ca^{++}. J. Physiol. 224: 317-332.

Kordas, M. 1972b. An attempt at an analysis of the factors determining the time course of the end-plate current. II. Temperature. J. Physiol. 224: 333-348.

Koshland, D.E. and K.E. Neet. 1968. The catalytic and regulatory properties of enzymes. Ann. Rev. Biochem. 37: 359-410.

Koshland, D.E., G. Nemethy, and D. Filmer. 1966. Comparison of experimental binding data and theoretical models in proteins containing subunits. Biochem. 8: 365-385.

Kuffler, S.W. and D. Yoshikami. 1975a. The distribution of acetylcholine sensitivity at the post-synaptic membrane of vertebrate skeletal twitch muscles. J. Physiol. 244: 703-730.

Kuffler, S.W. and D. Yoshikami. 1975b. The number of transmitter molecules in a quantum. J. Physiol. 251: 265-282.

Lassignal, N. and A.R. Martin. 1976. Reversal of acetylcholine potentials in eel electroplaque. Science 191: 464-466.

Lassignal, N. and A.R. Martin. 1977. Effect of acetylcholine on post-junctional membrane permeability in eel electroplaque. J. Gen. Physiol. 70: 23-36.

Lester, H.A. 1970. Spontaneous miniature synaptic potentials and quantal release of acetylcholine in skate electroplaques. Biol. Bull. 139: 428-429.

Lester, H.A. 1972. Blockade of acetylcholine receptors by cobra toxin: electrophysiological studies. Mol. Pharmacol. 8: 623-631.

Lester, H.A. 1977a. Sodium replaces internal K during bath application of cholinergic agonists to Electrophorus electroplaques. Biophys. J. 17: 133a.

Lester, H.A. 1977b. The response to acetylcholine. Sci. Am. 236: 106-118.

Lester, H.A., J.P. Changeux, and R.E. Sheridan. 1975. Conductance increases produced by bath application of cholinergic agonists to Electrophorus electroplaques. J. Gen. Physiol. 65: 797-816.

Lester, H.A., D.D. Koblin, and R.E. Sheridan. 1976. The acetylcholine concentration in the synaptic cleft during nicotinic transmission. Neurosci. Abst. 2: 714.

Llinas, R., R.W. Jayner, and C. Nicholson. 1974. Equilibrium potential for the postsynaptic response in the squid giant synapse. J. Gen. Physiol. 64: 519-535.

Magazanik, L.G. and F. Vyskocil. 1970. Dependence of acetylcholine desensitization on the membrane potential of frog fibre and on the ionic changes in the medium. J. Physiol. 210: 507-518.

Magazanik, L.G. and F. Vyskocil. 1975. The effect of temperature on desensitization kinetics at the post-synaptic membrane of the frog muscle fiber. J. Physiol. 249: 285-300.

Magleby, K.L. and C.F. Stevens. 1972a. The effect of voltage on the time course of end-plate currents. J. Physiol. 223: 151-171.

Magleby, K.L. and C.F. Stevens. 1972b. A quantitative description of end-plate currents. J. Physiol. 223: 173-197.

Malcolm, A.D.B. 1975. Biochemical applications of relaxation kinetics. Prog. Biophys. Molec. Biol. 30: 205-225.

Moreau, M. and J.P. Changeux. 1976. Studies on the electrogenic action of acetylcholine with Torpedo marmorata electric organ. J. Molec. Biol. 106: 457-467.

Nakamura, Y., S. Nakajima, and H. Grundfest. 1965. Analysis of spike electrogenesis and depolarizing K inactivation in electroplaques of Electrophorus electricus. J. Gen. Physiol. 49: 321-349.

Neher, E. and B. Sakmann, 1975. Voltage-dependence of drug-induced conductance in frog neuromuscular junction. Proc. Natl. Acad. Sci. USA 72: 2140-2144.

Neher, E. and B. Sakmann. 1976. Single-channel currents recorded from membrane of denervated frog muscle fibers. Nature 260: 799-802.

Neumann, E. and H.W. Chang. 1976. Dynamic properties of isolated acetylcholine receptor protein. Proc. Natl. Acad. Sci. USA 73: 3994-3998.

Popot, J.L., H. Sugiyama, and J.P. Changeux. 1976. Studies on the electrogenic action of acetylcholine with Torpedo marmorata electric organ. J. Molec. Biol. 106: 469-483.

Raftery, M.A., R.L. Vandlen, K.L. Reed, and T. Lee. 1975. Characterization of Torpedo californica acetylcholine receptor: its subunit composition and ligand-binding properties. C.S.H. Symposia 40: 193-202.

Ruiz-Manresa, F. and H. Grundfest. 1971. Synaptic electrogenesis in eel electroplaques. J. Gen. Physiol. 57: 71-92.

Ruiz-Manresa, F., A.C. Ruarte, T.L. Schwartz, and H. Grundfest. 1970. Potassium inactivation and impedance changes during spike electrogenesis in eel electroplaques. J. Gen. Physiol. 55: 33-47.

Schoffeniels, E. 1958. A method for studying separately the properties of the innervated and noninnervated membrane of an isolated single electroplax of the skate. Nature 181: 287-288.

Schoffeniels, E. and D. Nachmanson. 1957. An isolated single electroplax preparation. Biochem. Biophys. ACTA 26: 1-21.

Scubon-Mulieri, B. and R.L. Parsons. 1977. Desensitization and recovery at the frog neuromuscular junction. J. Gen. Physiol. 69: 431-447.

Sheridan, R.E. and H.A. Lester. 1975. Relaxation measurements on the acetylcholine receptor. Proc. Natl. Acad. Sci. USA 72: 3496-3500.

Sheridan, R.E. and H.A. Lester. 1977. Rates and equilibria at the acetylcholine receptor of Electrophorus electroplaques: a study of neurally evoked postsynaptic currents and of voltage-jump relaxations. J. Gen. Physiol. 70: 187-219.

Stevens, C.F. 1972. Inferences about membrane properties from electrical noise measurements. Biophys. J. 12: 1028-1047.

Weber, M. and J.P. Changeux. 1974a. Binding of Naja nigricollis (^{3}H) α-toxin to membrane fragments from Electrophorus and Torpedo electric organs. I. Binding of the tritiated α-toxin in the absence of effector. Molec. Pharmacol. 10: 1-14.

Weber, M. and J.P. Changeux. 1974b. Binding of Naja nigricollis (^{3}H) α-toxin to membrane fragments from Electrophorus and Torpedo electric organs. II. Effect of the cholinergic agonists and antagonists on the binding of the tritiated α-toxin. Molec. Pharmacol. 10: 15-34.

Weill, C.L., M.C. McNamee, and A. Karlin. 1974. Affinity-labeling of purified acetylcholine receptor from Torpedo californica. Biochem. Biophys. Res. Comm. 61: 997-1003.

Zingsheim, H.P. and E. Neher. 1974. The equivalence of fluctuation analysis and chemical relaxation measurements: a kinetic study of ion pore formation in thin lipid membranes. Biophys. Chem. 2: 197-207.